SUBSIDENCE, COMPACTION, AND THERMAL HISTORY OF SEDIMENTS IN THE NORTHERN NORTH SEA

by

MARIE DIANE SCHNEIDER

B.S., Yale University
(1979)

SUBMITTED TO THE DEPARTMENT OF
EARTH AND PLANETARY SCIENCES IN
FULFILLMENT OF THE REQUIREMENTS
FOR THE DEGREE OF

MASTER OF SCIENCE

at the

MASSACHUSETTS INSTITUTE OF TECHNOLOGY

June 1982

Signature of Author. . . . . .
Department of Earth and Planetary Sciences
May 29, 1982

Certified by . . . . . .
Dr. John G. Sclater
Thesis Supervisor

Accepted by. . . . . .
Dr. Theodore Madden
Chairman, Department Committee

SUBSIDENCE, COMPACTION, AND THERMAL HISTORY OF SEDIMENTS IN THE NORTHERN NORTH SEA

by

MARIE DIANE SCHNEIDER

Submitted to the Department of Earth and Planetary Sciences
on May 29, 1982 in partial fulfillment of the requirements
for the Degree of Master of Science in Earth and Planetary Sciences

ABSTRACT

The junction of the Viking, Central, and Moray Firth Grabens in the North Sea is an area which has been well-studied. Access to the lithological and geophysical logs of well 15/30-1 allowed a detailed interpretation of lithology and porosity to the Middle Jurassic. From the observed porosity-depth relations of the component lithologies, and applying compaction and sealing theories, the porosity history of the layers was inferred and used to compute thermal conductivity and sediment density of a layer with time. The compaction history was also used in conjunction with sea level curves and published (Wood, 1981) palynologically-derived deposition depths for the well to compute basement post-stretching subsidence due to thermal contraction corrected for loading effects. Flexural resistance and non-instantaneous stretching were ignored. This subsidence was matched with empirical subsidence curves for stretching rates and a stretching factor deduced. The current heat flow in the area was derived from computed conductivity to the depth of a measured and adjusted Bottom Hole Temperature of the well. This value was found to match the heat flow from the stretching model. This amount of stretching agrees with the amount of extension required by crustal thinning and recent subsidence in Ziegler's (1978) interpretation of a seismic profile across the Viking Graben.

The heat flow history since termination of fault-controlled subsidence, along with calculated conductivity of each layer through time may be used to derive the temperature history of a layer. Thus, temperature, porosity and bulk fluid flow from compaction are known with time. Applications of this method include hydrocarbon level-of-maturation calculations for a designated potential source layer, chemical equilibria and solution/diagenesis potential through time, and correlation of sealing times and fluid migration. Two special applications were considered: the level of maturity of the Upper Jurassic shale through time; and the timing of sealing of a high porosity-sand with oil shows.

Thesis Supervisor: Dr. John G. Sclater

Title: Professor of Marine Geophysics

Some moments later when he emerges hopeless from the tower to re-enter life again, we are not sure whether his decision is foredoomed and inescapable or an act of free will. We only know that amidst the stench and diversions of matter a tremendous spiritual struggle is in progress. Yet haunting our ears also throughout the book is the utterance of Maskull's mysterious supernatural companion: "The music was not playing for you, my friend."

Loren Eisely

Introduction to
Voyage to Arcturus
by David Lindsay

Acknowledgements

To Conoco for access to well logs and data, and particularly Walter C. Pusey III who got me started on my thesis with a very pleasant lunch.

To John Sclater, whose relaxed and optimistic approach went considerably to inspiring most of this work.

To John Hunt who helped me with his discussion and gave me some excellent leads.

To Professor James Eliot whose kind award of an MMRRI Scholarship supported my stay at M.I.T.

To the Ms. Eaglesfield and the librarians in Lindgren, who showed admirable patience and were always able to get me the refences I needed.

Also, credit must be given to:

Wardrobe, furnished by LL Bean and Matina Schneider

Gold card and telephone credit card provided by John Schneider

A Bergsonian glimpse of life, supplied by Laura Schneider

Jokes and good chile prepared (warmly) by Igor/the Puppy.

TABLE OF CONTENTS

I. Inferring the Compaction History of a Basin

It has been common practice to assume a constant and universal compaction curve showing the change of porosity with depth for a basic type of lithology (Sclater et al., 1980). A compilation of porosity-depth curves for shale (see Fig. 1) and carbonates (Fig. 2) from different areas indicates that the "principle" may not be the same in different locations. The universality through time has also been questioned by Van Elsberg (1980) for areas where sediment source or depositional environment have varied considerably. In the well studied, shale intervals with changing porosity trends show the same log porosity-depth slope, and the uppermost segment extrapolates to 62% porosity at sediment surface. Therefore for the dominant lithology, a single normal compaction principle can be assumed to apply before sealing takes place.

From the observed current porosity-depth relation and a consideration of principles of diagenesis and sealing, one may infer the way in which the porosity-depth plot changed with time.

A compilation of the effects of different sealing processes was made, in order to be able to identify probable sealing histories. In Fig. 3 the initial situation, history, and resulting porosity-depth curve are shown for five cases involving combinations of surface or at depth, complete or partial, and continuous or impulsive processes. When a seal is complete and at one level at one point in time, e.g. if "activation" or chemical sealing occurs at a tuff or hardground horizon, the portion below the seal is "frozen" into its porosity - stratigraphy relation. Unless there is subsequent re-partitioning of fluids in the mass, it is then buried with log-porosity-local depth relations it had at sealing time, while sediments over the seal may continue to compact.

A sealing process occurring at a certain depth, and over a period of time, will produce a buried segment of constant porosity. Partial seals which allow compaction but at a reduced rate will produce a steeper than normal log porosity-depth curve.

At any time, there is one zone in transition from normal-, to under-compaction. The time of transition for the base of a zone may be inferred today from the age of the layer which was at the surface when the zone under question was last on the normal compaction curve. This is done by accounting for the solid volume of sediments between the sealed zone and the surface at sealing time, in terms of current porosity for those overlying sediments. The procedure is outlined and porosity-depth relations worked out for important sealing times in Section VII. For the purposes of this study, eleven major intervals of porosity relations and composition were identified, stretching to 700 feet below well bottom. The sealing times in Section VII are the times at which the porosity-depth curve underwent a change of shape. For a time between these, one may derive the contemporaneous porosity-depth curve by selecting the sealing time previous to the time of interest, and adding normally compacting sediments to reach the surface at the datum layer.

In order to infer compaction history, it is necessary to make certain basic assumptions about sealing behavior. (To infer porosity histories, no assumptions have been made about which specific mechanisms operated to produce seals. Specific mechanisms which may have operated are described in Section II.)

The first assumption involves the slope and intercept of the normal compaction curve for shale, sands and carbonates. The normal curves are proposed to have the same exponential depth-dependence (slope of log-linear

curve) as currently observed in sealed sections. This involves two supporting assumptions: that a lithology type compacts at the same relation to depth of depth of burial through time; and that after a zone is sealed, there is no appreciable redistribution of fluids in the layer. From previous studies, the original near-surface porosity was set at 50% for sands (Chapman, 1973) and carbonates (Scholle, 1974) and the value of 62% for shale composition observed by Magara (1978) and others was found to agree with an extrapolation of the present uppermost porosity-depth relation to the surface.

A second major assumption was made in assuming that only complete sealing occurred and had either an impulse in time and depth dependence, or was effective at a particular depth, over a period of time. The third assumption is that mechanisms for porosity rejuvenation are not important.

The first and second assumptions are consistent with the currently observed shale log porosity-depth curve which consists of three parallel segments separated by constant porosity segments. See Fig. (5). Porosity may be increased in a sediment at depth by dissolution and microfracturing. These processes in general produce pore spaces which are detected by bulk density and neutron logs but not sonic logs, and thus may be quantitatively described. Such "secondary porosity" is observed (Fig. 6) to be less than 1-2%.

The fluid volume change involved in the smectite-illite transformation is positive (Whittaker et al., 1980) but the change in solid mineral volume probably reduces this effect (John Hunt, pers. comm.) (Gretener, 1979, p. 102). All porosity in the well is assumed to be primary and all porosity reduction final. Processes which might increase fluid pressure, such as aquathermal effect, are considered here as aids to maintaining a degree of

undercompaction but ineffective in increasing porosity. The increase in fluid pressure with burial is assumed to be only a result of increasing overburden (c.f. Palciauskas and Domenico). Scholle (1974) discusses low permeability of associated layers as leading to overpressures which brings about undercompaction by reducing effective stress and rate of pressure solution. In this paper, the low permeability is considered as the source of both overpressure and undercompaction. The reduction in dissolution rate is a reinforcing mechanism for maintaining high porosity, but the initial porosity is not considered to actually increase by this process.

II. Compaction Mechanisms and Sealing Mechanisms

Many processes have been described which can act to destroy or to preserve the original porosity of sediments, and some to create "secondary" porosity. Evidence for the relative importance of these processes and the ways they interact over geologic time-spans, is elusive. Some (e.g. Hedberg, 1936; Curtis, 1978) have produced the idea of universal, depth-related stages of sediment compaction based on the different porosity-depth relations observed at different levels in a particular basin. Others have questioned the need, or ability, to identify definite zones. The lithification of sediments is a wide-ranging and amorphous topic. Hinch (1980), Magara (1978) and Gretener (1981) have listed some of the major mechanisms affecting rate of porosity reduction, which are repeated here.

Mechanical compaction begins with the packing orientation of the grains due to their geometry, size distribution and environment of deposition. Particles of regular shape which have a wide size distribution and small mean size, and are deposited in agitated water will show densest

packing. Upon burial, anisotropic stress will contribute to breaking and rearrangement of grains. Mechanical compaction is dominant in the initial stages of burial, perhaps the upper 250 meters (Beall and Fisher, 1969).

Cementation of sediments may reduce porosity somewhat but in general preserves primary porosity, by strengthening the rock or by reducing permeability to chemical diagenetic agents and porefilling authigenic minerals. Cementation is an important lithification mechanism for sands. The succession of cementing materials in the North Sea Jurassic sands (Brent formation) has been well studied (e.g. Thomas, 1978). Silica cementation occurs early in burial history, requiring a source of silicate ions nearby, such as in fluids expelled from shales, and a low pH. The conditions for kaolinite formation (high poroperms, detrital illite, low pH and potassic feldspar material) were apparently met where kaolinite is observed at 840 feet in the well; the lignitic layers provide reducing conditions. Carbonate cementation in Brent sands generally post-dates kaolinite filling (Blanche and Whitaker, 1978), requiring high temperatures for precipitation (see below). Pore-filling by authigenic fibrous illite dramatically reduces permeability in the sands studied by Stalder (1973) by increasing tortuosity of fluid flow paths.

"Pressure" solution redistributes solutes primarily by grain boundary diffusion from sites of dissolution at points of contact and high stress to precipitation elsewhere. The mechanism is not well-defined and difficult to distinguish from recrystallization, and its low activation enthalpy makes it difficult to study in laboratory (Rutter, 1978). It is considered primarily in connection with carbonates, whose solution product increases as heating (e.g. burial) raises the pH of a solution (Siever, 1962).

Because diagenesis affects fluid flux and temperature by altering poroperm values and conductivity of rocks, there is a degree of feedback in the system. The situation also is complicated by the interaction of sediment layers of different lithology. Clay-rich seams in carbonates provide a path for chemical diffusion and appear to encourage solution transfer (Scholle, 1977); (Kennedy and Garrison, 1975).

The interaction of shale and sand layers has been studied by Magara (1978) and Fertl and Chilangar (1976). Undercompaction of shales at depth in many basins is often associated with rapid loading of a regressive phase. The sand content of the overlying sediments is often high, and Gretener (1981) has remarked that the loading of denser material may be the cause of the undercompaction. The effect of high sand or silt content in a sediment is to make it a preferential path for fluid migration with the result depicted in Fig. 4 and observed in many areas (Chapman, 1972). The layers with high clay content compact more readily, fluids being drained off or absorbed into the sandy layers. However, as observed by Chapman, the expulsion of water from shales is accompanied by plastic deformation and loss of permeability. After a time, for a certain scale of thicknesses, a clay-rich layer may "self-seal" to zero effective permeability on the boundaries but retain fluids at the center, which thereupon build up fluid pressure upon burial.

Compaction of sediments may proceed episodically with a pumping effect, and if the shales have been undercompacted this may occur at depth, providing efficient expulsion of the fluids (Gretener, 1981, p. 56). Magara (1978, p. 94-97) calculates critical permeability reduction to inhibit fluid expulsion for a certain rate of sedimentation and loading.

"Hardgrounds" in non-chalk limestones which form at or near the sediment surface (Hakansson, 1974) as well as "chemical rocks" (Price, 1976) which undergo extensive cementation at a certain depth, may comprise less than 5% of the layers but form impermeable barriers to fluid flow, and thus inhibit compaction. "Hardgrounds" have been correlated with sealevel drops and a consequent halt of accumulation (Scholle, 1977). Varying sediment composition or environments of deposition produce stratigraphic units which may be predisposed to a stage of pronounced porosity reduction at depth, as, for example, the "tight zone" at the Cretaceous-Tertiary boundary at Ekofisk, and the carbonate-cemented basal layers of sand depocycles at Brent (Taylor, 1978).

Porosity at depth may actually be increased by several processes. The term "secondary porosity" usually is used for micro-fracturing and solution cavities. Other processes such as aquathermal pressuring and smectite-illite transformation have also been considered as capable of increasing porosity in a layer. The carbonates which are "clean", low in clay and organic content, tend to fracture more readily (Bartok et al., 1981). Large grain size and low dolomite content also lower rock strength (Hugman et al., 1979). At Ekofisk, the anomalously high porosity levels of up to 40%, are partly due to microfracturing (Byrd, 1975); low lithic content, early cementation and burial has also resulted in extensive fracturing in the Austin Chalk (Wilson, 1976). Secondary porosity also includes solution vugs and cavities. The irregular shapes of secondary porosity cavities make them undetectable by sonic logs, while detected by bulk-density and neutron logging methods. This provides a means of determining the proportion of such secondary porosity when all three tools are used (Schlumberger, 1977).

The ability of the smectite-illite transformation to increase porosity at depth is not well documented; the sign of volume changes which would occur in the process not known (John Hunt, pers. comm.). The aquathermal effect of sealed water volume changes upon heating with burial are possibly an aid in maintaining high porosity brought about by other means (Gretener, 1981) but there is no evidence that this effect could actively introduce more porosity in basin sediments.

III. Note on Semantics

In the literature there appears to be some confusion over the relations between 1) high fluid pressures and undercompaction and 2) high thermal gradients and high porosity sediments.

1) In this study, the data relates to porosity or percent cavities detected to be filled by fluids. "Undercompaction" is a term used when divergence from a postulated normal compaction relation has been identified, and directly implies a greater than hydrostatic pressure for the fluids at depth. It must be remembered that greater-than-hydrostatic pressures may result from a variety of situations, and have been observed in very low porosity layers as well (Carstens and Dypvik, 1980). Since the purpose of this paper is to derive conductivity and fluid flux from porosity history, terms such as "overpressure" are avoided.

2) Several authors have noted the correlation of high "geothermal gradients" and undercompacted sediments (Selley, 1978, Magara, 1978). There are two sources of confusion here. First of all, a "geothermal gradient" as used in practice, is based on the change in temperature over a certain depth interval. Because sediment conductivities may vary considerably due to lithology and porosity differences (Robertson, 1979) the "geothermal gradient" may vary at one site depending on the level

sampled, or from place to place depending not on heat flow but on the conductivity differences. The level of sampling may also be important as focussing (lateral conductivity variations) or convecting effects (faults or permeable beds) may be more prevalent at a certain depth.

The second source of confusion lies in the chicken-and-egg relationship of high temperatures being conducive to chemical reactivity (possible solution or porosity maintaining effects), while at the same time high porosities are associated with lower sediment conductivities, resulting in higher geothermal gradients in an undercompacted section, as observed by Lewis and Rose (1970). The effect of porosity on the thermal conductivity of shale is not as dramatic as quartz content as Gretener observed (1981) from a consideration of the similar (low) conductivities of shale and water as compared with the very high conductivity of quartz. Thus, high geothermal gradients are associated with more quartz poor sections, which also will happen to have higher porosity reduction rates with depth. Before such a comparison is taken to infer the effect of a higher thermal gradient on porosity evolution (Selley, 1978) careful studies should be made on the variation in conductivity (and effects on the thermal gradient) due to variation in porosity and lithology.

IV. Log Interpretation of the Well

Access to a suite of logs of the Well 15/30-1 was generously provided by Conoco. Lithologic notes taken while drilling, and log analysis following methods outlined by Schlumberger (1977) and Dresser-Atlas (1975) manuals, were compiled and porosity and solid component determined for each level.

The porosities for most of the section were determined through crossplots of sonic, bulk density and compensated neutron logs, with "shale

points" determined every 500 feet. Care was taken to observe the effects of gas, lignite, tuffs and logging tool limitations and malfunctions. The lower 2000 feet of the section were analyzed from focussed and deep induction resistivity and gamma - SP logs.

In the upper 1800 feet of well section, a regular oscillation in sonic velocity was observed in cycles of around 40 feet. This periodic fluctuation, resembling Cousteau's (Toth, p. 152) "juvenile" basin is a result of differential compaction taking place at this level as described by Magara (1978, p. 46). The interpretation is that this level is composed of compacting layers alternating with layers which serve as conduits for the expressed fluids. For this section, following Magara (1978) mean porosities of the well-compacted layers are used for a determination of the "normal" trend of compaction with depth.

The Lower Cretaceous silty marls presented a problem in that too many variables of composition and porosity were present to accurately determine them. This zone is also very variable in porosity at each level (see Fig. 6). Porosity in carbonates can easily go down to zero in a layer since a solution transfer mechanism does not require external sources of water or solute (Scholle, 1977). Within major units, subunits important for conductivity calculations are also identified, where dolomite, tuff, or coal units are observed. Highly thermal-resistant layers are found to have an important effect on lowering the thermal gradient (see section X).

V. Summary of Well History Since the Jurassic

The following brief history of the well area, excerpted from Ziegler (1975); Kent (1975); Pegrum, Rees, and Naylor (1975); is a review of the events important in the evolution of the basin sediments. The history of subsidence in the area began in the Devonian and Early Carboniferous, when

the transformational folding of the Old Middle Old Red (Acadian) phase led to rapid subsidence in the Orcadian Basin and calc-alkaline volcanism in the vicinity of the well. In the Late Variscan orogeny, extensive wrench tectonism took place and "trapdoor basins" formed, filling with coal bearing strata and volcanics. The widespread development of faults at this and later periods is important to the assumption of fault-"controlled" initial, and subsequently the local isostatic thermal, subsidence (Kinsman, 1975). The updoming and dike swarms which occurred in the Forties and Egersund Basin at this time, and the subsequent major Triassic sedimentation, imply subcrustal attenuation. Dixon et al. (1975) have noted that in the light of the long relaxation time for lithosphere thermal perturbations (McKenzie, 1978) up to 100 m.y., these early stretching events may predispose the area to subsequent magma generation and then further subsidence.

In the Permian, subsidence resulted in 600 m of sedimentation of shale and sands, and it is suggested (Ziegler, 1981) that the Viking Graben began rifting at this time. In the Triassic the graben pattern developed on a large scale as pronounced rifting took place, but the low frequency of volcanics indicates that the stretching which took place was not yet localized. In the Early and Middle Jurassic, the ocean basins in the Atlantic began forming and as a result many basins in the area became inactive. Subsidence and sedimentation was interrupted by the mid-Cimmerian pulse which produced doming in the junction of the Central, Viking, and Moray Firth grabens, and volcanic flows at the center. The very rapid subsidence which followed allowed the deep-water organic-rich shales to be deposited on top of shallow-water sands. At this time, differential subsidence was taking place on rotational fault blocks, and

the lateral variation in thickness of organic shales and fan deposits of this age indicates relief on the order of one to two kilometers. The narrow, deep grabens formed were filled by clastics from the updomed Rockall and Shetlands Highs to the West.

Through the early Cretaceous, subsidence was faster than the sedimentation rate. Contemporaneous minor wrenching on the Great Glen Fault Zone indicate that the Moray Firth was still stretching. In the Late Cretaceous, steady, undisturbed subsidence set in. As spreading rates in the ocean went up and sea levels rose, clastic input from land surfaces was reduced, and chalks were deposited in deepening waters. Mesozoic rifting ended with the Paleogene onset of spreading on the Charlie Gibbs Fracture Zone. Most faults died out except for movements on major faults in the Laramide.

In the late Danian, with Laramide tectonic activity and a drop in sea level, chalk deposition ended and deep water sands from the East Shetlands barrier and delta system were laid down. In the Eocene, clastic fill was from topographic highs in the East and Southeast. In the Oligocene, glacial effects on sea-level created disconformities. The increased rates of subsidence and sedimentation in the Miocene and Pliocene are attributed to more rapid sediment loading. Loading induced subsidence depends on: sealevels, which control the quantity of clastics eroded as well as the level to which sediments may accumulate in basins; the degree of surrounding relief; and on the potential for carbonate production and accumulation. The degree of sediment loading at this time may be deduced from the relative rate of sedimentation and mean sediment density (Table II). The loading rate increased considerably in the Miocene and Pliocene, and it is suggested (Wood, 1981) that the time of accelerated subsidence is

related to the onset of glaciation.

VI. Observed Present Porosity-Depth Relation

Eleven major units were delineated by changes in log porosity-depth slope or lithology (Fig. 5). The uppermost shale sequence, 500-7400 ft. (165-2430 m) consists of 5 subunits, three of "normal" compaction slope alternating with two constant-porosity segments. From 7400 to 9000 feet (2430-2950 m) an Upper Paleocene sand unit exhibits a fairly well defined porosity reduction with depth (Fig. 7). Beneath it, 1,200 feet (394 m) of Lower Paleocene-Upper Cretaceous chalk follows a log linear porosity reduction with depth to a depth of 10,200 feet (3345 m) below sea level (Fig. 6). A marly limestone section below that shows great variation in porosity. A slope continuing the overlying chalk was picked for the upper 500 feet (165 m) and a constant porosity of 7% for the lower 1500 feet (490 m). 400 feet (130 m) of sand Albian/Aptian, with a constant 22% porosity overlie a lower Cretaceous silty marl with variable porosity, averaging 10%. At 13,700 feet below sea level (4495 m) the Upper Jurassic "Kimmeridge" hot E shale shows a porosity of around 24%. Below this level, for purposes of decompaction calculations to 100 Ma ago, the Jurassic series was considered to be similar to the description of Piper Field (Maher, 1980); porosity was assumed to be around 20%.

Porosity depth relations are summarized by Figures 5, 6, and 7 and Table III.

VII. Sealing Time Calculations and Porosity Evolution of the Well

In order to derive subsidence due to thermal contraction after stretching, the Aptian/Albian unconformity at 100 mybp is chosen as the time of onset of steady thermal subsidence. The most recent differential fault movement occurred in the nearby Piper Field in the Campanian at

around 70 mybp (Kent, 1975) but this is an anomalously late fault movement and in general no fault movement is observed in the area after 100 mybp. Therefore, the sediment compaction histories which are of interest begin with the layer 14,700 feet below s.l. (4,820 m). Calculations (see Table I) show that layers below this were sealed by 100 mybp.

Two forms of solving porosity equations are involved in deriving age of sealing (the present depth of a layer which was at surface when a layer under study was sealed). These are based on an assumption that the bulk solid volume in a time unit is conserved, and the difference between this volume (one dimensional because only vertical compaction is involved) and the layer thickness represents porosity. A sample calculation is carried out below; complete derivations of sealing time for various layers are presented in Table I.

Example

To get the beginning time of sealing for a layer A at current depth z_A (to its base) it is assumed that the porosity at this level represents the porosity at which it departed from a normal compaction curve. This porosity corresponds to a level z_{Ao} on the normal compaction relation. Between z_{Ao} and z = surface, sediments at the time of sealing (t=o) were on normal compaction curve. The proportion of solid in each layer today (S_A) is derived from its porosity relation ($\phi_A = F_A e^{-cz}$) and total thickness ($z_A - z_B$):

$$S_A = (z_A - z_B)(1 - \int_{z_A}^{z_B} F_{Ao} e^{-cz} dz), \qquad (I)$$

and then added over z_{Ao} after expansion to a normal porosity relation, to reach to a level z_{Bo} (solve for z_{Bo}):

$$S_A = S_{Ao} = \int_{z_{Ao}}^{z_{Bo}} (1 - F_{Ao} e^{-cz}) dz \qquad (II)$$

The process is repeated until the "decompacted" layers reach the surface. The final bit needs to be calculated by equation (I) to find the precise level of deposition at t=0.

Then this amount of solid is placed over its current base at its current porosity relation by solving for z_n as in equation (II).

This level corresponds to the age of sealing of A.

VIII. Subsidence Calculation

The basement subsidence compensated for local isostatic loading is calculated by

$$Y = S^* \left(\frac{(\rho_m-\rho_s)}{(\rho_m-\rho_w)}\right) + W_d - \Delta SL \left(\frac{\rho_m}{(\rho_m-\rho_w)}\right)$$

where ρ_m is the average mantle density, ρ_w is the average water density, and ρ_s is the average sediment density. Y is the depth to basement without sediment and water loads and represents the subsidence caused by "tectonic" effects. S^* is the sediment thickness corrected for compaction, W_d is the water depth at the time of deposition, and Δ_{SL} is the elevation of mean sea-level after Steckler and Watts (1978). A reference horizon of 14,700 feet below sea level was chosen as corresponding to the level of sealing and no further compaction beyond 100 mybp, the onset of steady thermally-controlled subsidence. The sediment thickness S to this depth was calculated after decompactin was applied (Table I) and sea levels estimated from Watts and Steckler (1979) were used. The depths of deposition for this well were studied by Wood (1981) from micropaleontological analysis. Final estimates range widely (0.3-1 km) for the 60-30 mybp period. The controversial nature of basinal chalk depth estimates were reviewed by Scholle (1974, p. 180-181), who found 200-500 m depths to be most in accord with all lines of evidence. For this period,

an estimate of 500 m was used. The sediment density for each thickness S of sediment was approximated by solid density of 2.65 (g/cm^3) weighted by integrated porosity containing water with density 1.1 (g/cm^3). The tabulated subsidence corrected for sediment and water loading is listed under Y_{corr} in Table II.

The resulting subsidence curves are shown in Figures 8a and 8b. Figure 8a shows the effect of each correction on the subsidence history; Figure 8b compares the loading-corrected subsidence curves with the calculated thermal subsidence for a stretching by a factor of 2.0, from Sclater and Christie (1981).

The observed subsidence curve matches the curve of predicted thermal subsidence upon stretching by a factor of 2.0, for a model based on instantaneous stretching. The stretching event in this case is believed to have lasted around 50 m.y. and isolated faulting events took place into the Upper Cretaceous in nearby sites, so the observed subsidence may include fault-"controlled" subsidence (due to replacing lithosphere by denser aesthenospheric material during stretching).

IX. Discussion of High Apparent Stretching Factor

Because the site is at the junction of the Central Viking, and Moray Firth Grabens, and in the vicinity of the large outpourings of middle Jurassic alkali olivine basalts (Howitt et al., 1975) (Dixon et al., 1980), it may be expected to show the maximum amount of stretching-induced thermal subsidence observed across the region. The well is also near the junction of the Fair-Isle Elbe line and the Highland Boundary Fault, an area of faulting and oblique-slip movement since the Hercynian (Late Carboniferous) orogeny (Threlfall, 1981). It is thus possibly predisposed to lower loading resistance during fault-controlled subsidence, which may have

persisted beyond 100 mybp as at the Piper Field (Kent, 1975). The need to infer a stretching factor of 2.0 during one stretching event (from 140-100 mybp) may be mitigated somewhat by considering a continuing effect of the previous attenuation, responsible for the extensive Triassic sedimentation in the area (Ziegler, 1978). Also, a part of the subsidence observed may be seen to be concentrated in an acceleration of the subsidence rate during the early Paleocene, associated with the Laramide tectonic activity, possibly another stretching episode.

X. Conductivity, Heat Flow, and Temperatures Through Time

From the composition and porosity relations of the log analysis and the following equation

$$\sum_{i=1}^{n} f_i \left[\frac{2}{3} + \frac{1}{3}\frac{K_i}{K}\right]^{-1} = 1 \qquad (1)$$

given by Henderson and Davis (1982) after Budiansky (1970), thermal conductivities of each lithologic unit were derived. The expression above has been derived by analogy to the electrostatic problem of a random mixture of n isotropic components in proportion f_i with conductivity K_i. An n-layered aggregate with layer thickness S_j and conductivities K_j has conductivity

$$K_m = \frac{\sum_{j=1}^{n} S_j}{\sum_{j=1}^{n} S_j/K_j} \qquad (2)$$

Conductivity end-member values used are listed in Table III, Notes (from Robertson (1979)).

The two expressions above and the Woodside-Messmer (1961) relation are compared in Figure 9, for a hypothetical combination of materials with conductivities 1.0 and 10.0. The insulating effect of a thin low conductivity layer in the laminated case is important; for this reason tuff layers such as the Eocene tephra in the well were noted and included in all conductivity and temperature calculations. Although generally similar, conductivities from equation (1) show slower dips to the low end member than the Woodside-Messmer empirically derived, geometric-mean relation. A preliminary check on values plotted in Robertson's (1979) thorough analysis of conductivities showed agreement with equation (1), and in view of its more physical basis it is used here. Values for marl, shale and sands compare well with Kappelmeyer et al. (1974).

The conductivities of the sediments through time are listed in Table III. Recent published thermal gradients (Evans and Coleman, 1974) show a gradient of 42°/1000 m. in the vicinity of the well. A thermogram of bottom hole temperatures corrected for disequilibrium from the Viking Trough (Carstens et al., 1981) is shown in Figure 10; Owen (1972) also reports a temperature recorded in nearby Ekofisk of 90° at 2.3 km. In the well 15/30-1, at 14,000 feet, a recorded temperature of 127°C was adjusted according to the mean correction suggested by Nwachukwu (1976) for time since mud circulation (12 hours) to equal 156°C. These four sources of temperature measurements at depth were matched to the tabulated thermal conductivities for the well and imply a heat flow of around 60 mW/m^2 (1.43 $\mu cal/cm^2 s$). This is close to the value predicted by a stretching of β = 2.0, 59 mW/m^2 (1.41 $\mu cal/cm^2 s$), 100 mybp after instantaneous stretching

(Sclater and Christie, 1980).

The thermal gradient curve deduced for the present shows a steepening (lower gradient) in the carbonate sediments, as predictable from their low porosity and high conductivity relative to more clay rich Tertiary sediments. There is a further shallowing of the curve (higher gradient) at the beginning of the Jurassic, as was observed by Cornelius (1975) and depicted by Carstens and Finstad (1981) for thermograms of the North Sea. The relatively low conductivity of Jurassic sediments is due to their better preservation of porosity, which counteracts the high conductivity of their large sand component. Cretaceous marls, on the other hand, show variable porosity (Scholle, 1977) but generally low values.

A correlation of high-porosity shales and high geothermal gradients in the Gulf Coast was interpreted by Lewis and Rose (1970) as a lowering of sediment conductivity due to large water content. Gretener (1981) states that this may not be an adequate explanation of the primary cause for low conductivities, considering the similar (low) conductivities of clay (1.48 $W/msec^2$) and water (.66). An alternative explanation was that the sand content of some shales is high enough to allow fluid release, lowering porosity, and raising sediment conductivity by its own contribution of a very high conductivity component (8.3).

The present heat flow value was extrapolated back in time for the heat-flow evolution depicted in Sclater and Christie, 1980, (Fig. 2) for a stretching of 2. As explained later in this paper, this predicted evolution of heat flow from higher values in the past has little effect on the thermal maturation of hydrocarbons in the Jurassic Shale. In conjunction with conductivity histories for each layer in Table III, temperatures for each layer were calculated using a sea-sediment interface

temperature of 0°C. The resulting thermograms down to the reference Jurassic level are shown in Figure 11. For a particular horizon one may determine the temperature history, as for the Jurassic "Kimmeridge" shale (next section).

This analysis ignores the effects of thermal disequilibrium upon rapid burial, temporary thermal anomalies of an intrusion in the vicinity, the focusing of heat flow due to lateral variation in conductivity, and heat loss to fluid flowing on faults or permeable strata or undergoing mass transport from compaction of sediments.

The thermal adjustment of a basin after an "instantaneous" accumulation of 13 km of sediments was calculated by Grossling (1959). He found that in the basin, thermal adjustment takes place quickly and near-equilibrium conditions are gained for the upper 20-30 km after 50 mybp, while the crust and lithosphere below this level take much longer to adjust. The rate of sedimentation in the well area seems not to have exceeded 100 m./m.y. so near-equilibrium conditions may be assumed to hold for the basin.

The thermal anomaly due to a magma intrusion has been studied by Lovering (1935) and Rititake (1959) and others. The change in thermal gradient 2 km or more from a molten body at 1300°C is a short-lived event, one which may be important for irreversible processes with high activation energies, such as hydrocarbon evolution or certain sediment diagenesis paths. The effect of a boost in the thermal gradient on hydrocarbon maturation is particularly strong when superimposed on the high temperatures of deep burial (Gretener, 1981), because of the exponential increase of the rate constant in the Arrhenius equation.

Lateral variations in conductivity in the vicinity of the well may result from stratigraphic changes in the sediments, porosity variation across the structural highs, or the block faulting -displaced sediments. The scales involved here make it unlikely that such variations are large enough to focus or defocus more than 5% of the heat flow (Jones and Oxburgh, 1979).

Thermograms constructed from bottom-hole temperatures from wells in the Northern North Sea characteristically show a kink in the thermal gradient which passes from high to low to high. This is often explained (Evans, 1970) as the effect of different conductivities of sediments comprising these three zones.

However, Cornelius (1975) showed that "curved" thermograms can result from fluid flow transporting some of the heat, with convex-upward thermograms indicating a seal near the top, and concave upward curves associated with a flushed zone. In the North Sea, high thermal gradients are reported on structural highs, and were interpreted by Carstens and Finstad (1981) as not due to conductivity variations in the structural highs but a result of fluid migration directed over the highs, either on faults or along permeable strata in tilted blocks. Faults are generally considered to be seals or barriers to flow at shallow depths, since authigenic quartz, clay, anhydrite and dolomite form an impermeable seal in the fault (Glennie et al., 1978). However, Price (1976) and Hubbert and Rubey (1959) showed that under conditions of high fluid pressure, the relative movement of faults could be facilitated. In the Gulf Coast, fluid pressures approaching geostatic are observed near low-angle faults (Bruce, 1972). Other evidence for fluid flow occurring on, or near (brecciated areas of) the fault zone include Fertl and Timko's and others' (in Price,

1976) studies of salinity in West Texas fields. These analyses indicate that there may be fresh water (from shale filtration at depth) migrating up distinct fault planes to the reservoirs. Werner and Doebl (1974) cited in Gretener (1981), found that geothermal gradients of wells in the Rhine Graben which are situated near faults, show a strong rise beyond any expected value of focussing due to high-conductivity fault block uplift. The amount of thermal gradient perturbation, that may be due to fault zone fluid migration is problematical; the assumption that in the long term it is negligible may be in error.

The fluid flow which occurs along permeable strata interlayered with less permeable layers (Magara, 1978) is here assumed to stop below sealing level. The effect of this flow on horizontal temperature gradients is assumed to be small, considering that tilting of the block on which the well is situated does not extend beyond the low porosity Upper Cretaceous layers which terminate in low porosity Paleocene sands.

Isotherms of paleotemperatures derived in Section X were superimposed on depositional histories of the sediments beginning with 140 mybp (Fig. 12). Three factors affect the subsurface temperature grid: heat flow, lithology (solid) conductivity, and degree of compaction (filling pore space with low-conductivity fluids). The compacted and carbonate-rich Cretaceous segment which causes a lower geothermal gradient in its vicinity (Fig. 12, "C") is seen to have caused a spreading in the isotherms since it began compacting beyond around 4000 feet (13% porosity) below sediment surface. A simplified version of this phenomenon is presented in Fig. 13.

Bonham (1980) considered the effects of a changing geothermal gradient in relation to the fluid flux resulting from sediment compaction during subsidence. For sediments compacting uniformly to zero porosity on a

typical (log-linear) porosity loss curve, fluid flux will be downward ("pre-equilibrium") or upward ("post-equilibrium") relative to a constant sea level. A changing geothermal gradient with time may then enhance or retard the heating of sediments as they are buried, and have various effects on the fluid flux depending on the specific rates and values involved.

If a sealing effect is introduced, as at level B on Fig. 13, the fluid flux in a sediment will be once again downward with increasing burial. The seal may be assumed for this level of analysis to be complete (see Magara, 1978, p. 169 for discussion) and the fluids contained will be subjected to the same temperature history as the sediments.

XI. Example One: Thermal History of Upper Jurassic Shale

The methods outlined above are of particular interest in relation to the calculation of level of maturation for possible petroleum source beds. The accumulated L.O.M. as expressed by Gretener (1981) is one of many similar attempts to include time and temperature in hydrocarbon evolution:

$$TF = \frac{1}{1000} T_o \cdot 2^{\left(\frac{T-T_o}{10}\right)}$$

$$LOM = \Sigma(TF \cdot \text{exposure time in m.y}).$$

The L.O.M. required for intense oil generation has been estimated at 130 (Connan, 1974) to 700 (Hood *et al.*, 1975) with Tissot *et al.*'s level of 350 being close to the mean of most present estimates. The problem in defining an L.O.M. lies partly in the combination of chemical reactions important for a specific organic source material, with different reactions showing different rate relationships to temperature variation (Tissot *et al.*, 1978). Tissot and Welte (1978) found that Type II kerogen (on a Van Krevelen diagram) based on aromatic, marine source material and found in

the North Sea basin source rocks to have a lower L.O.M. requirement than other types. A comparison of activation energies of kerogen types is in Fig. 14. For the purposes of this study, an L.O.M. of 100 was considered as the oil-production threshold.

A graph of the temperature history (Fig. 15) and (accumulated) L.O.M. with time (Fig. 16, L.O.M.) of the "Kimmeridge-Callovian" upper Jurassic shale, shows that this occurrence of the shale reached an L.O.M. of 100 at around 25 mybp. The effects of the exponential increase in temperature factor make the time spent at low temperatures unimportant to the level of maturation of kerogen. Therefore, although heat flow may have been higher in the past according to the stretching model, this has little effect on the early, cool stages of burial of the Upper Jurassic Shale.

XII. Example Two: Porosity Evolution of Albian Sands

The Albian-stage sands at 12200 feet below sea level have a range of porosities, with some high values recorded. The oil shows at this level make it of interest to note the apparent sealing time in relation to the time of possible migration and porosity-affecting mechanisms.

Several studies of sediment diagenesis in relation to hydrocarbon occurrence have noted the evidence for a porosity-preserving effect of oil infiltration into e.g. sandstone (Hancock and Taylor, 1978), (Sommer, 1978) and chalk (Van den Bark et al., 1980). Oil infiltration may inhibit the pore-filling by permeability-reducing illite, as suggested by Stalder (1973). Or, organic content may act to lower pH and the degree of pressure solution of quartz (Blanche and Whitaker, 1978), or simply reduce silicate ion flux in the vicinity (Taylor, 1978b). The Albian sandy layers which occur around 12200 feet below sea level, have been calculated to have sealed around 69 mybp. (This was derived by the method outlined above:

current porosity (f) at this level was projected back onto a "normal" compaction curve (e.g. f'=f exp (-cz)); depth z for this porosity was found; sediments overlying the Albian were decompacted normally to the surface and the age of the final (top) layer taken to be the time of sealing.) If the oil shows at this level were involved in inhibiting compaction, the source was probably not in the Upper Jurassic shale beneath, which was not thermally mature before around 25 m.y. ago (Section XI). However, the Upper Jurassic shale is widely noted as having been deposited in rapidly deepening waters: it directly overlies the shallow water Oxfordian sands and smooths out horsts and grabens. The Lower Cretaceous silty marls overlying the shale also exhibit highly variable thicknesses as noted by Maher (1980). In order to reach the oil-generation stage by 69 m.y., a minimum of an extra 1200-1500 feet burial is required. This amount of differential sedimentation is observed at Piper Field (Maher, 1980) and may be presumed to lie in the Witch Ground graben close to the well. With regard to the time for oil migration to these sands, it is noted that the anomalously late fault movement which is observed in the Piper Field nearby occurred in the Campanian, around the time of sealing of the sand.

Perhaps active faults at this time were involved in oil migration. The mobility of fluids on fault zones may be facilitated by overpressuring as suggested by Hubbert and Rubey (1959) and Price (1976). Calculations show that overpressuring probably did exist at this level at 69 mybp: the average depth for sealing (beginning of undercompaction) appears to be around 3000-3500 feet below sediment surface; once sealed, sediments show steadily increasing fluid pressures upon burial (Fertl, 1979).

An alternative explanation for undercompaction at 12200 feet is suggested by the high-porosity shales in association with the high porosity sands at this level, similar to the situation in the Statfjord and Brent fields. Blanche and Whitaker (1978) suggest that "overpressuring" - or the development of high fluid pressure gradients upon burial after sealing - has preserved the sand porosities. The typical sealing depths of the local shale (around 3500 feet below sediment surface) and the sand (3700 feet) are similar and suggest that a situation such as depicted in Fig. 4 took place. The shale layers probably "sealed" before the sands and the fluid circulation from the clays was stopped, after which the sands stopped compacting. If the sand compaction involved pressure solution, as described by Blanche and Whitaker (1978), the pore water expelled from adjacent shales may have been an important source of silica replenishment after precipitation.

III. Conclusion

The correlation of tectonic events, paleotemperatures, and sealing history is possible by the methods described above and may be applied to many problems. A rigorous study of sediment diagenesis requires such information about temperatures, fluid flux and fluid pressures.

For example, higher temperatures tend to raise the pH of fluids at depth (Siever, 1962) (Bucke and Mankin, 1971) and this in turn would raise the calcium carbonate solubility product and promote precipitation of carbonate (Blanche and Whitaker, 1978). On the other hand, a low pH is important to effecting pressure solution of quartz, and higher temperatures may inhibit compaction by this mechanism.

A calculation of minimum permeability for fluid flow through sediments is possible if permeability reduction is assumed to be the sealing

mechanism (Magara (1978). It would be of interest to develop the same method for the flow of immiscible fluids using principles outlined by Bear (1972).

Finally, it appears that a network of effects conducive to hydrocarbon generation may be generated during the characteristic history of basin formation. The rates and types of sedimentation, structural geology and heat flow history observed in this area may be due to a common cause. The method of backstripping and deducing thermal and fluid flux history outlined above reveals some of the reinforcing or compensating effects of sedimentation rate and composition, heat flow history, and subsidence mechanisms.

References

Albright, W.A., Turner, W.L., and Williamson, K.R., "Ninian Field, North Sea" in Giant Oil and Gas Fields 1968-1978, AAPG Mem. 30, p. 173-193, (1980).

Bartok, P., Reijers, T.J.A., and Juhasz, I., "Lower Cretaceous Cogollo Group, Maracaibo Basin, Venezuela: sedimentology, diagenesis, and petrophysics" Bull. AAPG, vol. 65, p. 1110-1134, (1981).

Bear, J., Dynamics of Fluids in Porous Media, Elsevier, (1972).

Berggren, W.A. and Gradstein, F.M., "Agglutinated Benthonic Foraminiferal Assemblages..." in Petroleum Geology of the Continental Shelf of N.W. Europe, Illing and Hobson, eds., p. 282, (1981).

Blanche, J.B. and J.H. Whitaker, "Diagenesis of Brent Sand Formation", J.G.S. London, 135, p. 73-82, (1978).

Bonham, L.C., "Migration of Hydrocarbons in Compacting Basins", Bull. AAPG, 64, p. 549-567, (1980).

Bradley, J.S., "Abnormal Formation Pressure", AAPG Bull. 59, p. 957-973, (1975).

Bruce, C.H., "Pressured Shale and Related Sediment Deformation", Gulf Coast Assoc. Geol. Socs. Trans., v. 22, p. 23-31, (1972).

Bucke, D.P., Jr., and Mankin, C.J., "Clay-mineral diagenesis within interlaminated shales and sandstones", J. Sed. Pet., 41, p. 971-981, (1971).

Budiansky, B., "Thermal and thermoelastic properties of isotropic composites", J. Composite Mat., 4, p. 286-295, (1970).

Byrd, W.D., "Geology of Ekofisk Field, Offshore Norway", in Petroleum and the Continental Shelf of Northwest Europe, Woodland, ed., p. 438, (1975).

Carstens, H. and Dypvik, H. "Abnormal formation pressure and shale porosity", Bull. AAPG, v. 64, p. 344-350, (1980).

Carstens, H. and Finstad, K.G., "Geothermal gradients of northern North Sea basin", in Petroleum Geology of the Continental Shelf of North-West Europe, Illing and Hobson, ed., (1981).

Chapman, R.E., Petroleum Geology, Elsevier, 285 pp., (1973).

Chilingar, G., Mannon, R., and Rieke, H., III, Oil and Gas Production from Carbonate Rocks, N.Y.: Elsevier, 396 pp., (1972).

Christie, P.A.F. and Sclater, J.G., "An extensional origin for the Buchan and Witchground Graben in the North Sea", Nature, London, 283, p. 729-732, (1980).

Clarke, R.H., "Cainozoic subsidence in the North Sea", EPSL, 18, p. 329-332, (1973).

Connan, J., "Time temperature relation in oil genesis", Bull. AAPG, 58/12, p. 2516-2521, (1976).

Cornelius, C.D., "Geothermal aspects of hydrocarbon exploration in the North Sea" in Norges Geologiske Undersokelske, Nr. 316, ed. Whiteman, A., et al., p. 29, (1975).

Curtis, C.D., "Possible links between sandstone diagenesis and depth-related geochemical reactions occurring in enclosing mudstones," J.G.S. London 135, p. 107-117, (1978).

Dixon, J.E., Fitton, J.G. and Frost, R.T.C., "The tectonic significance of Post-Carboniferous igneous activity in the N. Sea Basin", in Pet. Geol. of the Cont. Shelf of N.W. Europe, Illings and Habson, eds., Pet. Inst. London, p. 121, (1981).

Dresser-Atlas, Log Interpretation Fundamentals, Dresser Atlas, (1975).

du Rouchet, J.H., Stress Fields, A Key to Oil Migration; AAPG 65/1, p. 74-85, (1981).

Evans, T.R., "Thermal Properties of North Sea Rocks", The Log Analyst, March, 1970.

Evans, T.R., and Coleman, N.C., "North Sea Geothermal Gradients", Nature, 247, p. 28-30, 1974.

Fertl, W.H., Abnormal Formation Pressures, Developments in Petroleum Sci. Ser. #2, Elsevier, (1976).

Fischer, A.G., and Judson, S., eds., Petroleum and Global Tectonics, Princeton: Princeton U. Press, 322 pp., (1975).

Fuchtbaeur, H., Die Sandstein diagenese im Spiegel der neueren Literatur", Geol. Rundschau, 68/3, p. 1125-1151, (1979).

Glennie, Mudd, and Nachtegaal, "Depositional environment and diagenesis of Permian Rotliegendes Sandstones in Leman block and Sole Pit areas of the U.K. Southern North Sea" JGS, London 135, p. 25, (1978).

Gretener, P.E., Pore Pressure - Fundamentals, General Ramifications and Implications for Structural Geology, AAPG Cont. Ed. Course Notes Ser. #4, 2nd ed'n, 131 pp., (1979).

Gretener, P.E., Geothermics: Using Temperature in Hydrocarbon Exploration Ed. Short Course Note Ser. #17, AAPG, (1981).

Grossling, B.F., "Temperature Variations Due to the Formation of a Geosyncline", GSA 70/10, p. 1253-1281, (1959).

Hancock, N.J., "Possible causes of Rotliegend sandstone diagenesis in northern West Germany", J.G.S. London 135, p. 35, (1978a).

Hancock, N.J. and Taylor, A.M., "Clay mineral diagenesis and oil migration in the Middle Jurassic Brent Formation", JGS London 135, p. 69-72, (1978).

Hakansson, E., Bromley, R. and Perch-Nielsen, K., "Maastrichtian chalk of North-West Europe", in Pelagic Sediments, Hsu and Jenkyns, eds., (1974).

Hedberg, H.D., "Gravitational compaction of clays and shales", Am. J. Sci., 31, p. 241-287, (1936).

Henderson, J.R. and Davis, E., "An estimate of heat flow in Western North Atlantic at DSDP Site 54", in press.

Heritier, F.E., Lossel, P., and Wathne, E., "Frigg Field: Large Submarine Fan-Trap...", in Giant Oil and Gas Fields: 1968-1978, AAPG Mem. 30, p. 59-79, (1980).

Hill, P.J. and Wood, G.V., Forties Field, North Sea", in Giant Oil and Gas Fields: 1968-1978, AAPG Mem. 30, p. 80-93, (1980).

Hinch, H.H., "The Nature of Shales and the Dynamics of Hydrocarbon Expulsion in the Gulf Coast Tertiary Section", AAPG Studies in Geology No. 10: Problems of Petroleum Migration, Roberts and Cordell, eds. p. 1-18, (1980).

Howitt, F., Aston, E. and Jacque, M., "The occurrence of Jurassic volcanics in the North Sea", in A.W. Woodland (ed.) Petroleum and the Continental Shelf of North West Europe, Vol. I, London, p. 379-387, (1975).

Hubbert, M.K. and Rubey, W.W., "Role of fluid pressure in the mechanics of overthrust faulting," GSA 70/2, p. 115-166, (1959).

Hugman, R.H.H., III, and Friedman, M., "Effects of texture and compositon on mechanical behavior of experimentally deformed carbonate rocks", Bull. AAPG, 63, p. 1478-1489, (1979).

Hunt, J.M., Petroleum Geochemistry and Geology, Freeman, 617 pp., (1979).

Jackson, K.C., Textbook of Lithology, New York, McGraw-Hill, 528 pp., (1970).

Jarvis, G.T., and McKenzie, D.P., "Sedimentary basin formation with finite extension rates", EPSL, 48, p. 42 (1980).

Jones, F.W., and Oxburgh, E.R., "Two-dimensional thermal conductivity anomalies and vertical heat flow variations", in Terrestrial Heat Flow in Europe, (eds. V. Cermak and L. Ryback) Springer, Berlin, p. 98-106, (1979).

Jones, P.H., "Role of geopressure in hydrocarbon and water system", AAPG Studies in Geology #10, Roberts and Cordell, ed., p. 207-216, (1980).

Kappelmeyer, O. and Haenel, R., Geothermics With Special Reference to Application, Geoexplor. Monographs Ser. 1, No. 4, 234 pp., (1974).

Kent, P.E., "Review of North Sea Basin Development", J.G.S. London, 131, p. 435-468, (1975).

Kennedy, W.J., and Garrison, R.E., Morphology and genesis of nodular chalks and hardgrounds in the Upper Cretaceous of S. England", Sed. v. 22, p. 311-386, (1975).

Kinsman, D.J., "Rift valley basins and sedimentary history of trailing continental margins", in Petroleum and Global Tectonics, Fischer and Judson, eds., Princeton, p. 83-125, (1975).

Kirk, R.H., "Statfjord Field - A North Sea Giant", in Giant Oil and Gas Fields 1968-1978, AAPG Mem. 30, p. 95-116, (1980).

Lewis, C.R. and Rose, S.C., A theory relating high temperatures and over-pressures, J. Pet. Tech., 22: 11-16, (1970).

Lovering, T.S., "Theory of heat conduction applied to geological problems", GSA 46/1, p. 69-93, (1935).

Magara, K., Compaction and Fluid Migration, Developments in Petroleum Science 9, Elsevier, New York, 319 pp., (1978).

_____. "Discussion - "A New Approach to Sediment Diagenesis by J. Van Elsberg", Bull. Can. Pet. Geo. 28, 2, p. 290-295, (1980a).

_____. "Agents for Primary Hydrocarbon Migration: A Review", in AAPG Studies in Geology No. 10: Problems of Petroleum Migration, p. 33-45, (1980b).

_____. "Static vs. Dynamic Interpretation in Petroleum Geology", Bull. AAPG, v. 65, p. 531, (1981).

Maher, C.E., "The Piper Oil Field", Ch. 33 in Petroleum Geol. of the Continental Shelf of NW Europe, Illing and Hobson, eds., p. 358-370, (1981).

McKenzie, D.P., "Some remarks on the development of sedimentary basins", EPSL, 40, p. 25-32, (1978).

Nagtegaal, P.J.C., "Sandstone framework instability as a function of burial diagenesis", J.G.S. London 135, p. 101-105, (1978).

Neugebauer, J., "Some aspects of sedimentation in chalk", in: Pelagic sediments: on land and under the sea (Hsu and Jenkyns, eds.), Spec. Publs. Int. Ass. Sedement 1, p. 149-176, (1974).

Nwachukwu, S.O., "Approximate geothermal gradients in Niger Delta sedimentary basin", Bull. AAPG 60, 1073-1077, (1976).

Owen, J.D., "Log analysis of Ekofisk Field", Petroleum Engineer, p. 58, Nov. (1972).

Oxburgh, E.R. and C.P. Andrews-Speed, "Temperatures, thermal gradients and heat flow in the southwestern North Sea", Chill in Petroleum Geo. of the Continental Shelf of N.W. Europe, Illing and Hobson, eds., Inst. Pet. London, p. 141-151, (1981).

Palciauskaas, V. and Domenico, P., "Microfracture development in compacting sediments: relation to hydrocarbon - maturation kinetics", Bull. AAPG, 69, p. 927-937, (1980).

Pegrum, R.M., Rees, G., and Naylor, D., Geology of the North-West European Continental Shelf, Vol. 2, London, 1975.

Pirson, S.J., Geologic Well Log Analysis: 2nd ed., Gulf Publishing Co., 377 pp., (1977).

Price, L.C., "Aqueous solubility of petroleum as applied to its origin and primary migration", Bull. AAPG, 60, p. 213-244, (1976).

Rititake, T., "Studies of the thermal state of the Earth, part 2 - Heat flow associated with Magma intrusions", Bull. Earthquake Research Inst. Tokyo, 32/2, p. 1584-1596, (1959).

Robertson, E.C., "Thermal conductivities of rocks", USGS Open File Report 79-356, (1979).

Rutter, E.H., "Discussion on pressure solution", in J.G.S. London, 135 pp., (1978).

Schlumberger Log Interpretation Charts, 1977 ed.

_____ Log Interpretation Vol. I: Principles; Vol. II: Intrepretation.

Scholle, P.A., "Diagenesis of Upper Cretaceous chalks from England, Ireland and the North Sea", in Pelagic Sediments: On Land and Under the Sea, Hsu, K.J. and Jenkyns, H.C., ed.; Blackwell Sci. Pub., Oxford, 1974.

Scholle, P.A., "Chalk diagenesis and its relation to petroleum generation: oil from chalks, a Modern Miracle?", Bull. AAPG, 61, p. 982-1009, (1977).

Sclater, J.G. and Christie, P.A.F., "Continental stretching: An explanation of the Post mid-Cretaceous subsidence of the Central North Sea Basin", JGR, 85, p. 3711-3739, (1980).

Selley, R.C., "Porosity gradients of North Sea Oil-Bearing Sandstones", J.G.S. London, 135, p. 133-135, (1978).

Siever, R., "Silica solubility, 0-200°, and diagenesis of siliceous sediments", J. Geol., 70, p. 127-150, (1962).

Snowdon, L., "Errors in extrapolation of experimental kinetic parameters to organic geochemical systems", Bull. AAPG, 63, p. 1128-1138, (1979).

Sommer, F., "Diagenesis of Jurassic sandsones in the Viking graben", J.G.S. London, 135, p. 63-67, (1978).

Stalder, P.J., "Influence of crystallographic habit and aggregate structure of Authigenic clay minerals on sandstone permeability", Geologie en Mijnbouw, 52, p. 217-220, (1973).

Steckler, M.S. and Watts, A.B., EPSL, 41, p. 1-13, (1978).

Taylor, J.C.M., "Control of diagenesis by depositional environment within a fluvial sandstone sequence in the northern North Sea Basin", JGS London, 135, p. 83-91, (1978).

Taylor, J.C.M., "Discussion on pressure solution", JGS London, 135, p. 134, (1978b).

Thomas, J.B., "Diagenetic sequences in low-permeability argillaceous sandstones", JGS London, 135, p. 93-99, (1978).

Thomas, J.B., Walmsley, P.J., and Jenkins, D., "Forties Field, North Sea", Bull. AAPG, 58, p. 396-406, (1974).

Threlfall, W.F., "Structural framework of the central and northern North Sea", in Petroleum Geology of the Continental shelf of N.W. Europe, Illing and Hobson, eds., p. 98, (1981).

Tissot, B.P. and Welte, D.H., Petroleum Formation and Occurrence, Springer-Verlag, 525 pp., (1978).

Tissot, B.P., Bard, J.F., and Espitalie, J., "Principal Factors Controlling the Timing of Petroleum Generation", CSPG Mem. #6, p. 143-152, (1980).

Toth, J., "Hydraulic theory of migration", in Problems of Petroleum Migration, Roberts, W.H., III, and Cardell, R.J., eds., AAPG Studies in Geology, No. 10, p. 121-168, (1980).

Van den Bark, E. and Thomas, O.D, "Ekofisk Field, North Sea", in Giant Oil and Gas Fields 1968-1978, AAPG Mem. 30, p. 195-224, (1980).

Van Elsberg, J.N., "Reply to discussion of 'A New Approach to Sediment Diagenesis", CSPG, 28, p. 292-295, (1980).

Waples, D., "Time and temperature in petroleum formation", AAPG 64/6, p. 916-926, (1980).

TABLE I

	Input	Compaction Relation	Calculation I or II	Output
Sealing begins for (2)	1. z=500 to z=2400	A	I	S=990
	2. z=2400 to z=3630	$\overline{.38}$	I	S=772
	3. S=990 - 772	A	II	z = 2035
Age of 2035 level; = 4 MYBP				
Sealing ends for (4)	1. z=500 to z=2674	A	I	S=1162
	2. z=3650 to z=5000	A'	I	S=907
	3. S=255	$\overline{.38}$	II	z=(3650 - 412)
Age of 3237 level; = 8 MYBP				
Sealing begins for (5)	1. z=2670 to z=3217	$\overline{.36}$	I	S=351
	2. z=500 to z=2670	A	I	S=1162
	3. S=(351+ 1162 - 641)	A'	II	z=3706
Age of 3706 level; = 21 MYBP				
Sealing begins for (6)	1. z=500 to z=3250	A	I	S=1545
	2. z=6000 to z=7400	A"	I	S=1021
	3. S=(1545 -1021)	$\overline{.36}$	II	z=5183
Age of 5183 level; = 33 MYBP				

TABLE I (cont.)

		Input	Compaction Relation	Calculation I or II	Output
Sealing begins for (6A)	1.	S=1524 z=4700	B	II	z=3083
	2.	z=500 to z=3083	A	I	S=1432
	3.	z=7400 to z=6000	A"	I	S=1021
				II	z=5360
Age of 5360 level; = 35 MYBP	4.	S=(1432-1021) z=6000	$\overline{.36}$		
Sealing begins for (9a)	1.	z=10700 to z=12200	$\overline{.07}$	I	S=1395
	2.	z=9000 to z=10700	C'	I	S=1536
	3.	S=(1395+1536)	C	II	z=3736
	4.	z=3736 to z=1254	B	II	z=1089
	5.	z=500 to z=1089	A	I	S=263
Age of 7050 level; = 51 MYBP	6.	S=263 z=7400	A"	II	z=7070
Sealing begins for (9b)	1.	S=231 z=3583	B	II	z=3280
	2.	z=500 to z=3280	C	I	S=1870
	3.	S=(1870-1395) z=10700	C'	II	z=10185
Age of 10185 level; = 69 MYBP					

TABLE I (cont.)

		Input	Compaction Relation	Calculation I or II	Output
Sealing begins for (11)	1.	S=172 z=4320	B	II	z=4093
	2.	S=1100 z=4093	A	II	z=2500
	3.	z=500 to z=2500	C	I	S=1517
	4.	S=1517 z=1220	.07	II	z=10560
Age of 10560 level; = 75 MYBP					

Basement or sealed level at 95 MYBP:

Assume porosity of .22 (as at Piper Field) at z=14200 below sediment surface. At a depth of 4100 (d=4100; z=4100 + water depth) this layer was sealed. The corresponding levels above this layer at 100 MYBP are shown in Table III.

TABLE II. SUBSIDENCE CALCULATIONS

Age (MA)	Water Depth (Feet)	Sed. Density	(1) S	(2) Y	(3) -Δ Sealevel (meters)	(4) Y_{corr} (meters)
0	500	2.26	14300	2366	0	2366
4	500	2.30	12950	2095	0	2095
8	800	2.29	11870	2050	0	2050
21	800	2.31	10917	1874	20	1844
33	1500	2.26	9550	1973	100	1823
35	1500	2.28	9383	1920	100	1770
51	1500	2.33	8436	1713	130	1523
56	1500	2.33	7327	1552	135	1352
58	1500	2.29	6814	1518	140	1308
69	500	2.24	6780	1236	100	1086
75	500	2.21	4867	955	90	825
95	500	2.26	3750	745	20	715

(1)
S = sediment thickness to the shallowest fully compacted layer at 95 MYBP. in feet

(2)

$$Y = S \frac{\rho_m - \rho_s}{\rho_m - \rho_w} + \text{W.D.}$$

(3) Steckler-Watts' Sea Level Curve (meters)

(4) $Y_{corr} = Y - \Delta \text{ Sealevel } \left(\frac{\rho_m}{\rho_m - \rho_w}\right)$

TABLE III

LITHOLOGY (sh-ss-carb)	Present. Sea level=500 z (1)	Por. reln/ Ave. por.	k (2)	dT/dz (3)	T (4)	4 MYBP. Sea level=500 z	Por. reln/ Ave. por.	k	dT/dz	T	8 MYBP. Sea level=800 z	Por.reln/ Ave.por.	k	dT/dz	T
1. (85-.10-.05)	500	A/.48	1.15	52	32										
2. (.85-.10-.05)	2400	.382	1.30	46	51	500	A/.47	1.18	51	32	800	A/.53	1.11	54	14
3. (.75-.20-.10)	3650	A'/.45	1.39	43	70	2400	A/.33	1.62	42	50	1620	A/.42	1.44	42	33
4. (.70-.15-.15)	5000	.36	1.50	40	73	3750					2970				
4a. (.50-.30-0)	5220-5290	.36	1.86	32	74/77										
4b. (.50-.30-0)	5500-5600	.36	1.86	32	78/83						3470				
5. (.80-.05-.15)	6000	A"/.28	1.42	42	97	4750					3970				
5a. (.70-.10-.20)	7000-7400	A"/.28	1.51	40	102										
6. (.40-.60-0)	7400	B'/.21	3.45	17	105	6150					6370				
6a. (.10-.10-.80ch)	9000	C'/.12	2.96	20	109						6970				
7. (.10-.10-.80)	9500	C'/.10	2.82	21	113	7750					7470				
8. (.20-.05-.75)	10200	C'/.08	2.57	23	117	9500					8170				
9. (.20-.05-.75)	10700	.07	2.60	23	126	10950					8170				
9a. (.30-.10-.60dolo)	11900-12200	.07	3.58	17	128						8670				
9b. (.30-.40-.10)	12200-12500	.15-.23	2.55	24	130										
9c. (.80tuff-.10-.10)	12500-12600	.15	1.42	42	132										
10. (.80-.05-.15)	12600	.15	1.51	40	133	11350					10570				
10a. (.20-.80-0)	12700-12900	.14	6.2	10	134/144										
11. (1.0-0-0)	13700	.24	1.26	48	146	12450					10670				
J1	13800		1.3	46	150						11670				
J2	14100		2.2	30	151										
J3	14200		1.6	38	153										
J4	14300		1.3	46	154										
J5	14400		1.9	32	157										
(J6)	(14900)					(13450)					(12670)				

LITHOLOGY (sh-ss-carb)	21 MYBP, Sea level=800					33 MYBP, Sea level=1500					36 MYBP, Sea level=1500				
	(1) z	Por. reln/ Ave. por.	(2) k	(3) dT/dz	T	z	Por. reln/ Ave. por.	k	dT/dz	T		Por.reln/ Ave.por.	k	dT/dz	T
1. (85-.10-.05)															
2. (.85-.10-.05)	800	A/.57	1.06	60	6										
3. (.75-.20-.10)	1117	A/.46	1.36	57	27	1500	A/.57	1.06	60	7	1500	A/.60	1.02	63	4
4. (.70-.15-.15)	2517 2970	A/.36 .36	1.50	57	41	1850	A/.49	1.27	50	11	1700	A/.56	1.16	55	22
4a. (.50-.50-0)						2070- 2140	.49	1.75	36	12					
4b. (.50-.50-0)						2350- 2450	.49	1.75	36	16					
5. (.80-.05-.15)	3517					2850	A/.37	1.30	49	38	2700	A/.38	1.29	50	45
5a. (.70-.10-.20)	4917														
6. (.40-.60-0)	6517					4250	.22	3.45	18	48	4083	B/.22	3.50	18	54
6a. (.10-.10-.80ch)	7717					5850					5680				
7. (.10-.10-.80)	8217					6350					6183				
8. (.20-.05-.75)						7050					6883				
9. (.20-.05-.75)						7550					7383				
9a. (.30-.10-.60dolo)															
9b. (.50-.40-.10)															
9c. (.80tuff-.10-.10)															
10. (.80-.05-.15)	9617					8950					9283				
10a. .20-.80-0)															
11. (1.0-0-0)	10717					10050					10383				
J1															
J2															
J3															
J4															
J5															
(J6)	(11717)					(11050)					(11383)				

LITHOLOGY (sh-ss-carb)	51 MYBP. Sea level=1500					56 MYBP. Sea level=1500					69 MYBP. Sea level=1500				
	(1) s	Por. reln/ Ave. por.	(2) k	(3) dT/ds	(4) T	s	Por. reln/ Ave. por.	k	dT/ds	T	s	Por. reln/ Ave. por.	k	dT/ds	T
1. (85-.10-.05)															
2. (.85-.10-.05)															
3. (.75-.20-.10)															
4. (.70-.15-.15)															
4a. (.50-.50-0)															
4b. (.50-.50-0)															
5. (.80-.05-.15)	1500	A/.55	1.08	65	13										
5a. (.70-.10-.20)															
6. (.40-.60-0)	2143	B/.33	2.82	24	34	1500	B/.43	2.26							
6a. (.10-.10-.80ch)	4070	C/.16	2.68	25	38	2675	C/.27	2.25	31	17					
7. (.10-.10-.80)	4600	C/.13	2.81	24	42	3185	C/.26	2.40	29	25	1500	C/.46	1.69	28	6
8. (.20-.05-.75)	5400	C/.12	2.48	28	47	4050	C/.20	2.23	31	31	2000	C/.38	1.80	30	13
9. (.20-.05-.75)	5920	C/.09	2.57	26	57	4615	C/.13	2.43	29	48	2560	C/.24	2.12	28	30
9a. (.30-.10-.60dolo)															
9b. (.50-.40-.10)	7436					6330	.23	2.55		60	4280	B/.24	2.55	25	32
9c. (.80tuff-.10-.10)											4583				
10. (.80-.05-.15)	7836					6730									
10a. .20-.80-0)															
11. (1.0-0-0)	8936					7830									
J1															
J2															
J3															
J4															
J5															
(J6)	(9936)					(8830)					(6783)				

LITHOLOGY (sh-ss-carb)	75 MYBP. Sea level=500					95 MYBP. Sea level=500				
	(1) z	Por. reln/ Ave. por.	(2) k	(3) dT/dx	(4) T	z	Por. reln/ Ave. por.	k	dT/dx	T
1. (85-.10-.05)										
2. (.85-.10-.05)										
3. (.75-.20-.10)										
4. (.70-.15-.15)										
4a. (.50-.50-0)										
4b. (.50-.50-0)										
5. (.80-.05-.15)										
5a. (.70-.10-.20)										
6. (.40-.60-0)										
6a. (.10-.10-.80ch)										
7. (.10-.10-.80)										
8. (.20-.05-.75)										
9. (.20-.05-.75)	500	C/.32	1.80	42	31					
9a. (.30-.10-.60dolo)										
9b. (.50-.40-.10)	2500	B/.28	2.35	32	36	500	B/.49	1.75	42	7.5
9c. (.80tuff-.10-.10)						1000	C/.25	1.15	65	10
10. (.80-.05-.15)		A/.27	1.44	52	37	1100	A/.47	1.17	64	11
10a. .20-.80-0)	4090	B/.25	4.50	16	39	1200-1500	B/.42	3.35	22	14
11. (1.0-0-0)	4320	.24	1.26	60	54	3000	A/.35	1.15	65	50
							B/.25			
J1										
J2										
J3										
J4										
J5										
(J6)	(5367)					(4250)			64	73

TABLE III

NOTES

(1) z = depth below sea level to top of layer, in feet

(2) Porosity relation indicated for major lithological component (sh=shale, ss= sand, carb = carbonate, dolo= dolomite, ch= chalk):

sh $A = 0.6635 \times \exp(-.00023d)$

$A' = 0.8841 \times \exp(-.00023d)$

$A'' = 1.258 \times \exp(-.00023d)$

ss $B = 0.563 \times \exp(-.000238d)$

$B' = 1.51 \times \exp(-.000238d)$

carb $C = 0.589 \times \exp(-.00033d)$

$C' = 2.44 \times \exp(-.00033d)$

(3) K = thermal conductivity of sediment, in W/m°K , derived from:

$$\sum_i f_i \left(\frac{2}{3} + \frac{1}{3}\frac{K_i}{K}\right)^{-1} = 1$$

Component (i)	K_i's =	
	8.3	quartz
	1.5	clay
	0.66	hot water
	3.0	limestone
	3.3	chalk
	1.3	tuff
	5.0	dolomite

(4) T = temperature at base of layer, °C

(5) For all levels beneath "-------" in table, the porosity relations, conductivities, and thermal resistivities are as at present.

FIGURE 1

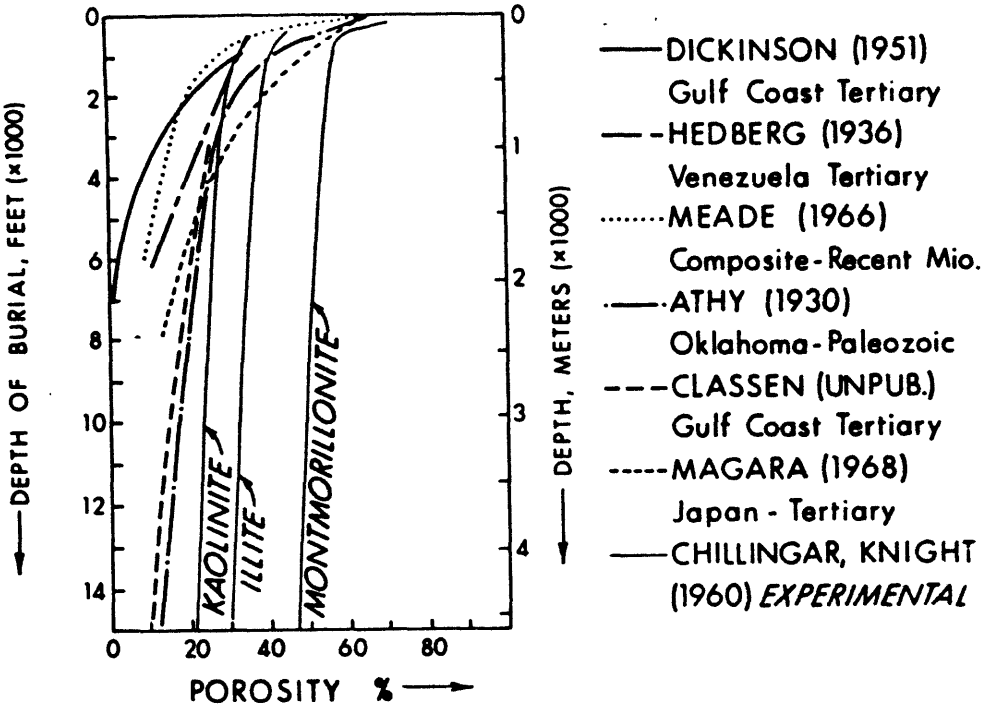

—Selected curves showing changes in shale porosity with depth.

FROM HINCH, (1980)

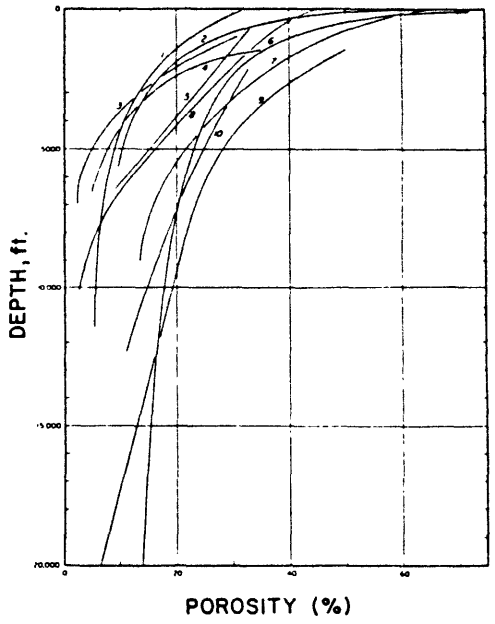

FROM MAGARA (1980)

—Relation between porosity and depth of burial for shales and argillaceous sediments (from Rieke and Chilingarian, 1974). Data plots: 1, Proshlyakov (1960), 2, Meade (1966); 3, Athy (1930); 4, Hosoi (1963); 5, Hedberg (1936), 6, Dickinson (1953); 7, Magara (1968a); 8, Weller (1959); 9, Ham (1966); and 10, Foster and Whalen (1966).

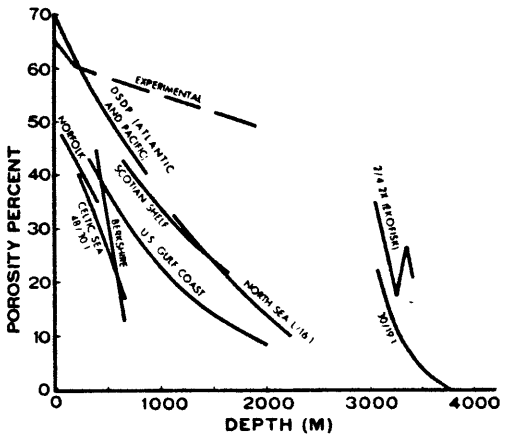

FIG. 2—Plot of porosity changes as function of burial depth in chalks.

from Scholle (1977).

Figure 3.

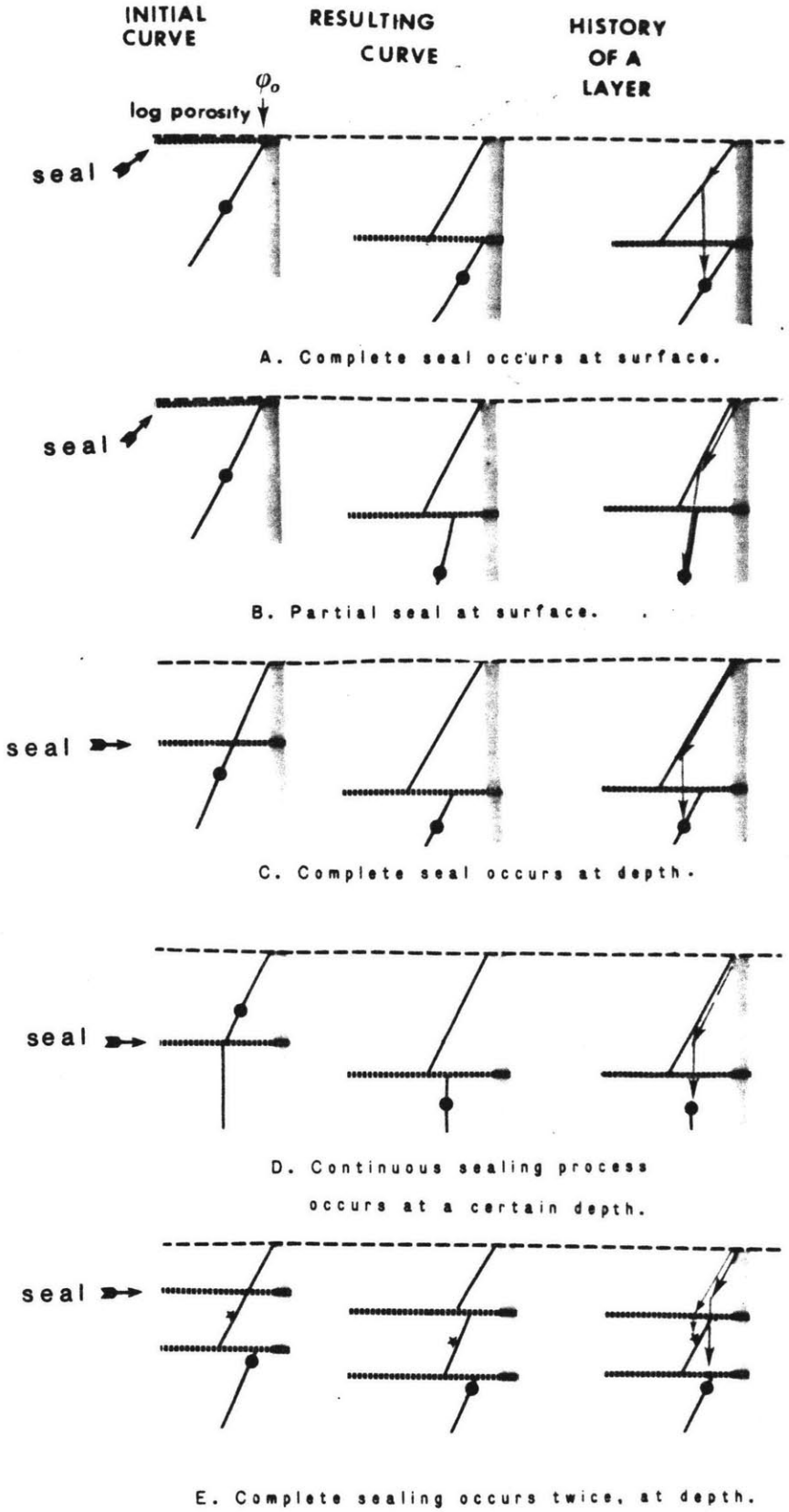
INITIAL CURVE
RESULTING CURVE
HISTORY OF A LAYER
φ_o
log porosity
seal
A. Complete seal occurs at surface.
seal
B. Partial seal at surface.
seal
C. Complete seal occurs at depth.
seal
D. Continuous sealing process occurs at a certain depth.
seal
E. Complete sealing occurs twice, at depth.

Figure 4. AFTER MAGARA (1980)

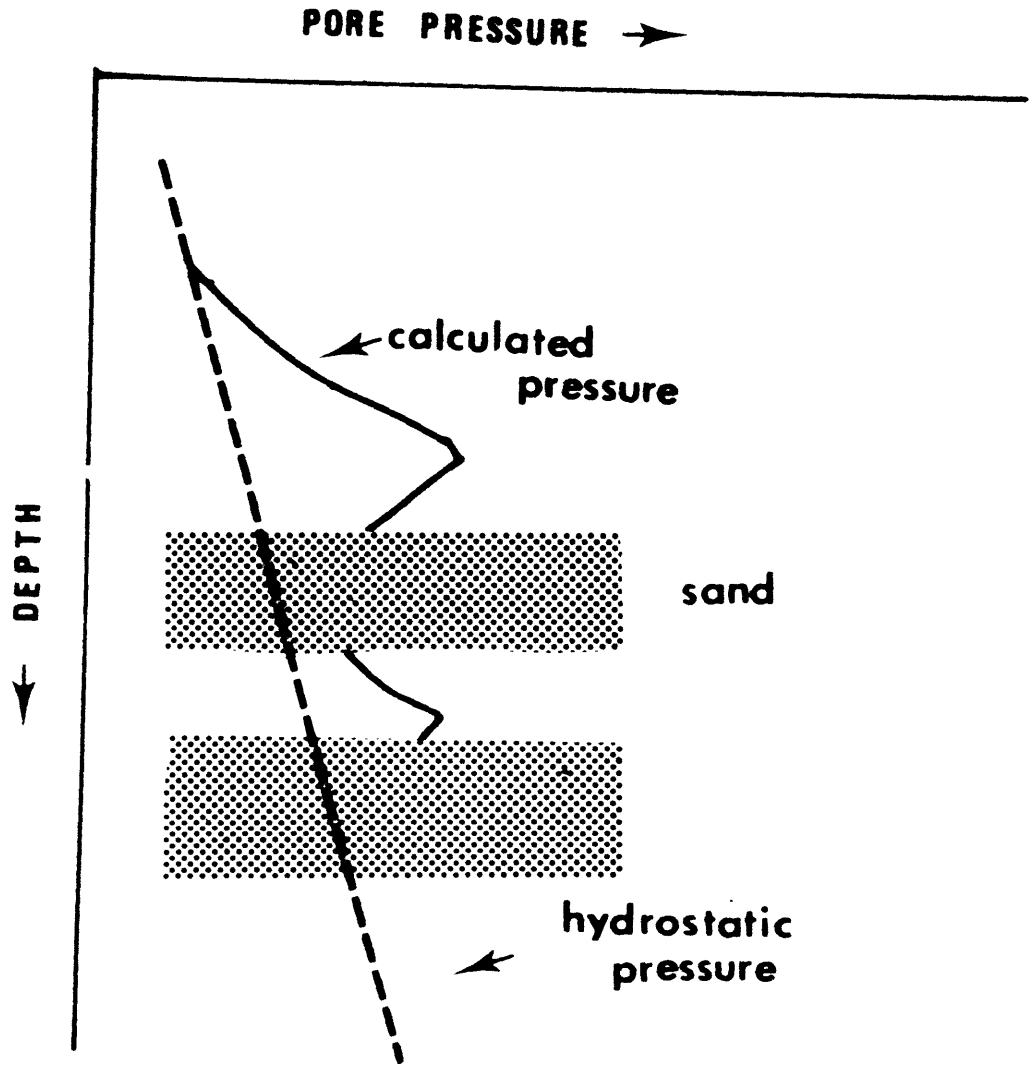

Figure 5. Lithology and log porosity (sonic log) for shale.

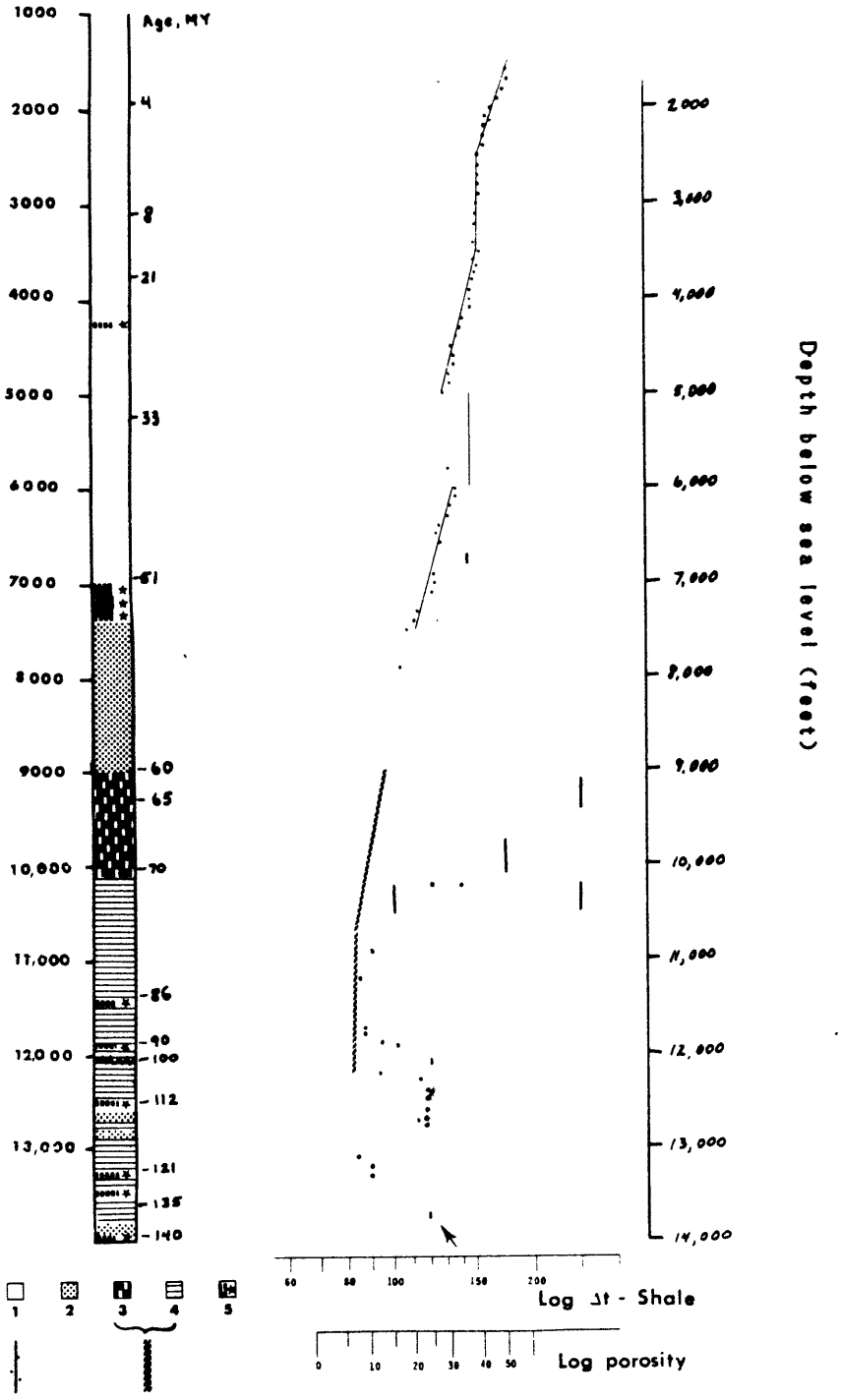

1 – shale 2 – sand 3 – chalk 4 – marl 5 – tuff

Sand porosity (gray) and carbonate (diagonal stripes) shown for reference.

Upper Jurassic Shale indicated by arrow.

Figure 6. Carbonate porosity-depth relation

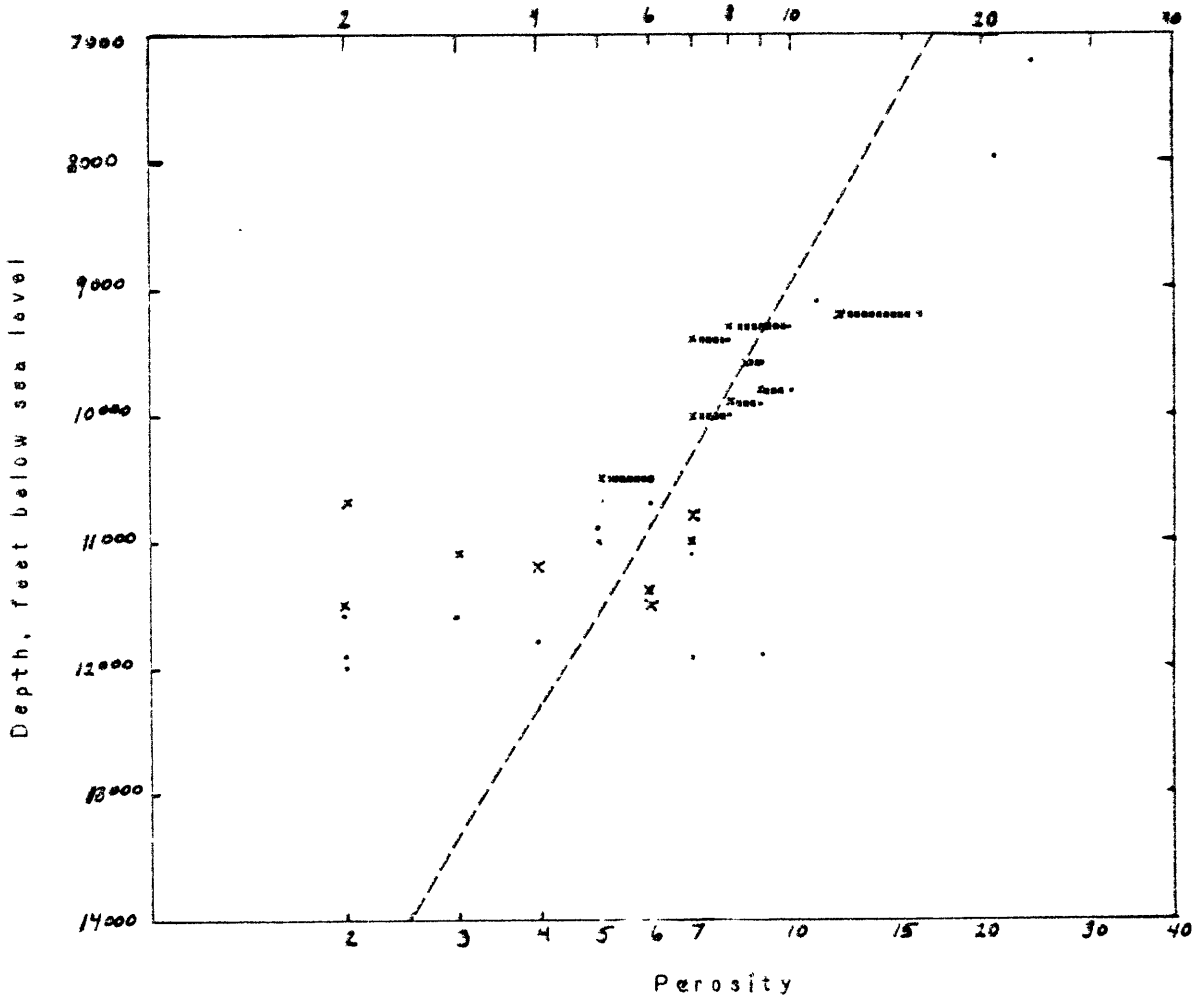

Figure 7.

Paleocene sand, log porosity–depth relation

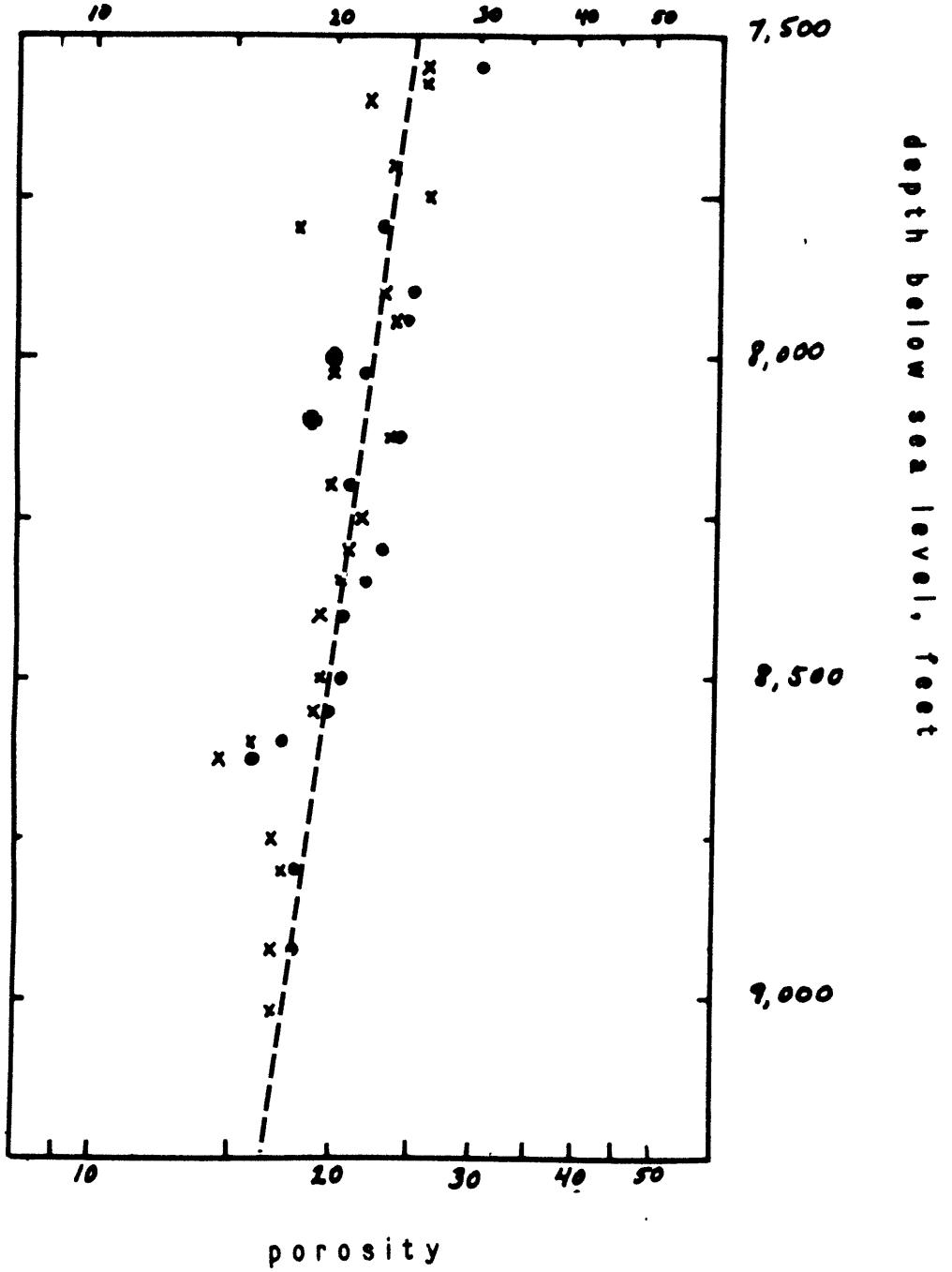

x: sonic–bulk density log crossplot

o: neutron–bulk density crossplot

Figure 8a.

Y_1 = Present change of thickness with age

decompacted with time

$Y_3 = Y_1\left(\frac{\rho_m - \rho_3}{\rho_m - \rho_w}\right)$

$Y_4 = Y_3 - W.D.$

$Y_5 = Y_4 - \Delta S.L. \frac{\rho_m}{\rho_m - \rho_w}$

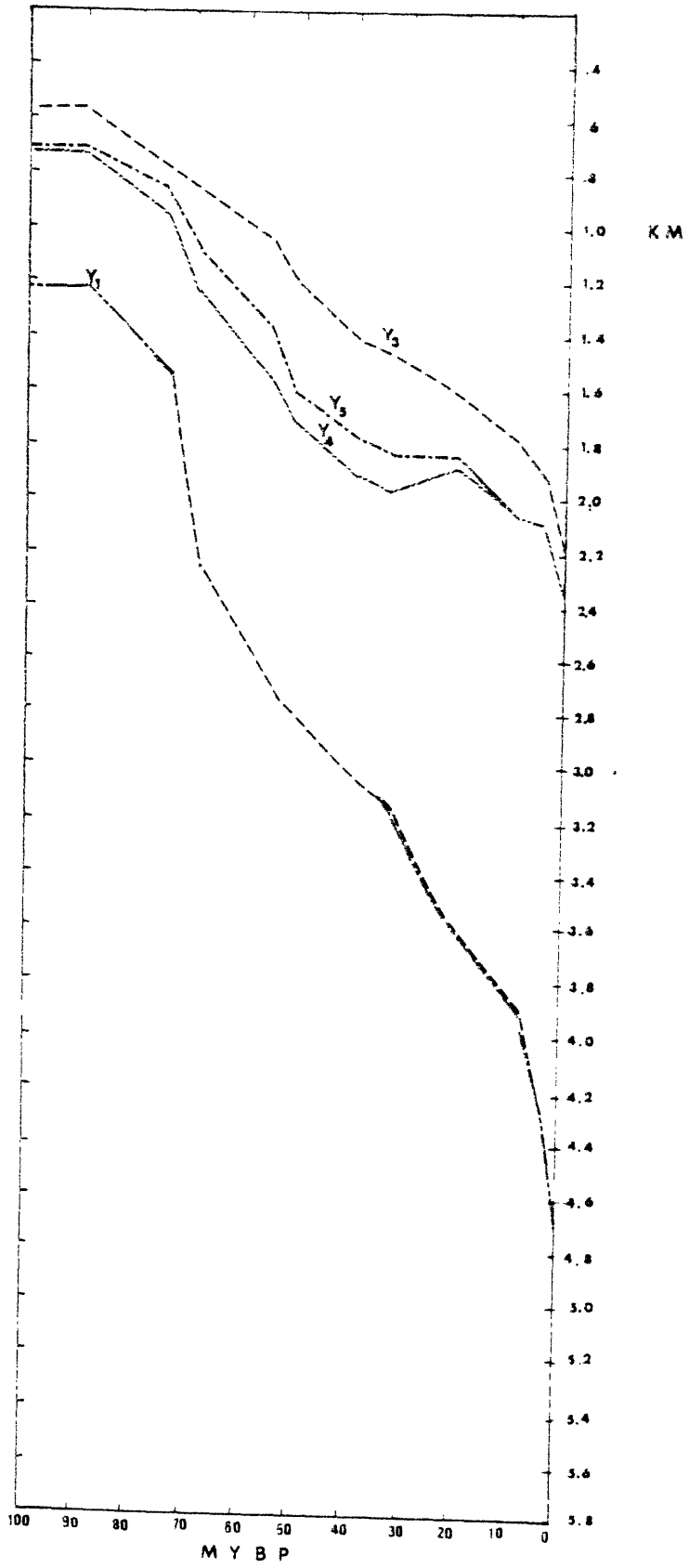

Figure 8b. Subsidence curves, with sediment loading, compaction, and water-depth correction.

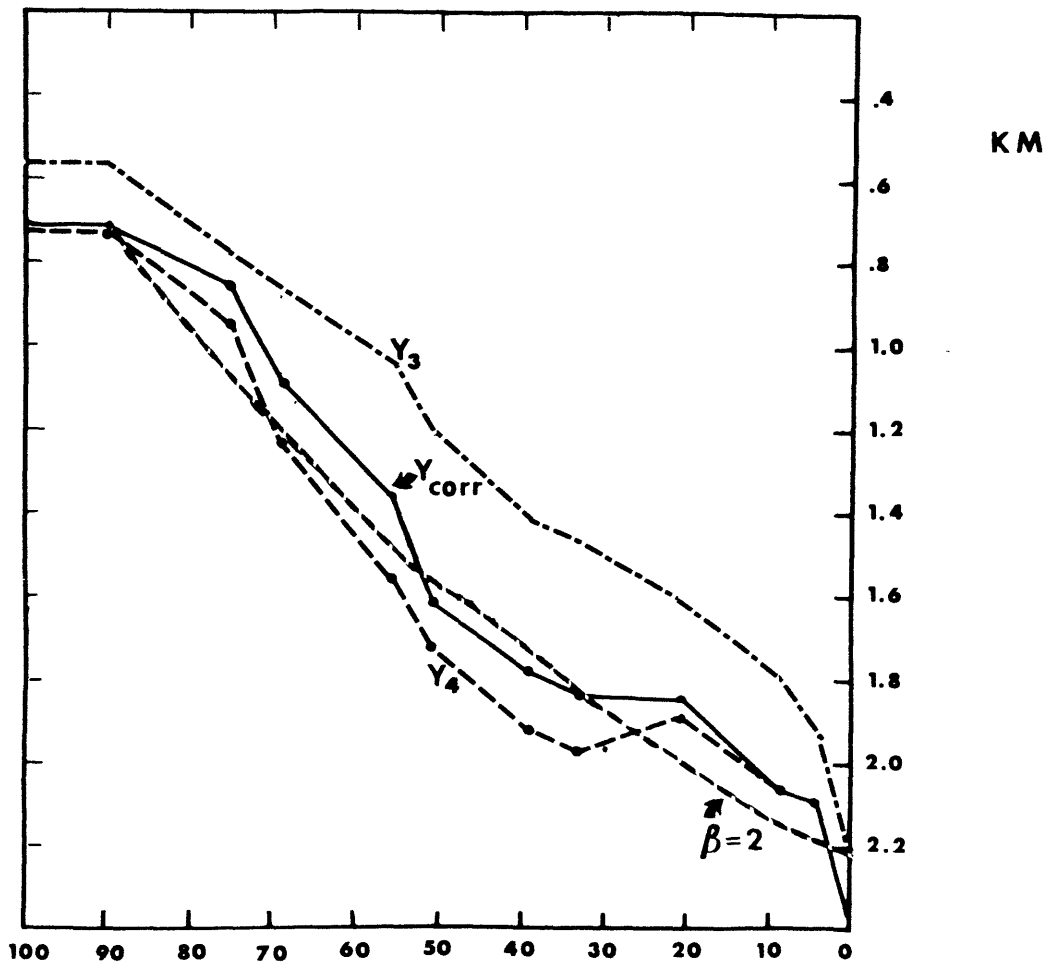

Y_3, Y_4: see Fig. 8a.

Y_{corr} : with Watts-Steckler sea level correction

$\beta=2$: predicted basement subsidence for stretching factor 2

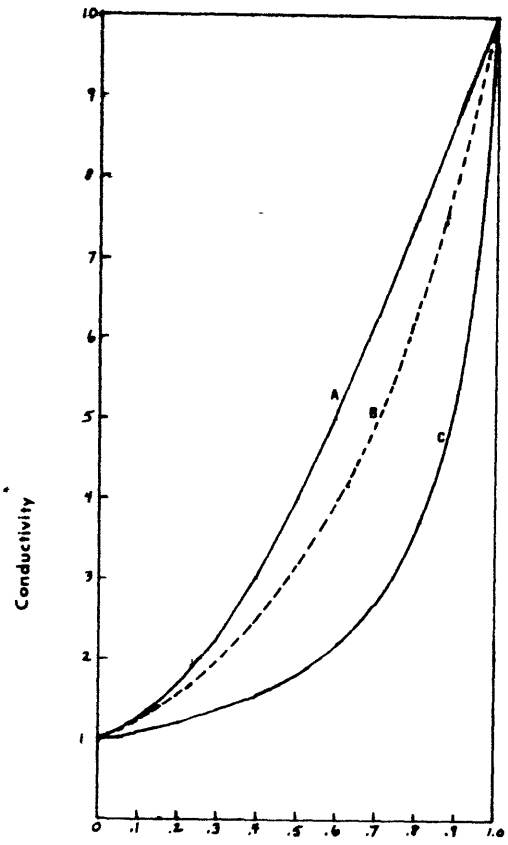

Figure 9

Comparison of conductivity of a composite material calculated three ways.
The composite is of two hypothetical materials, with thermal conductivities of 10 and 1.0.

A: Budiansky electrostatic analogy

B: Woodside and Messmer

C: Laminar mixture

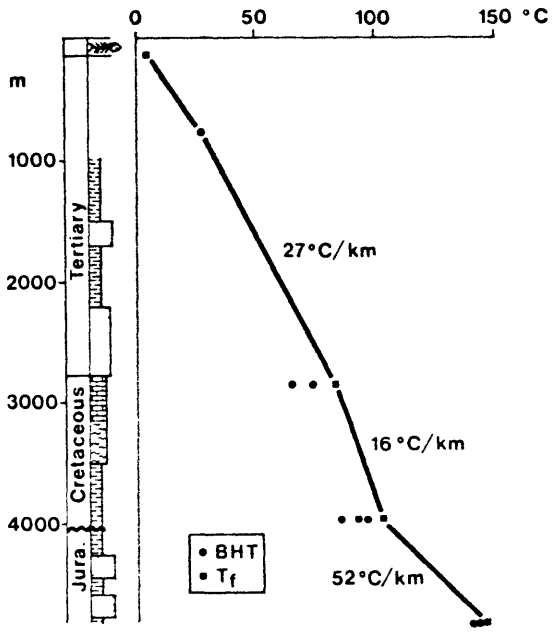

Fig. 10. Thermogram of a Viking Trough well. Note the marl and limestone of the Cretaceous sequence in this well.

from Carstens and Finstad (1981).

Figure 11 A.

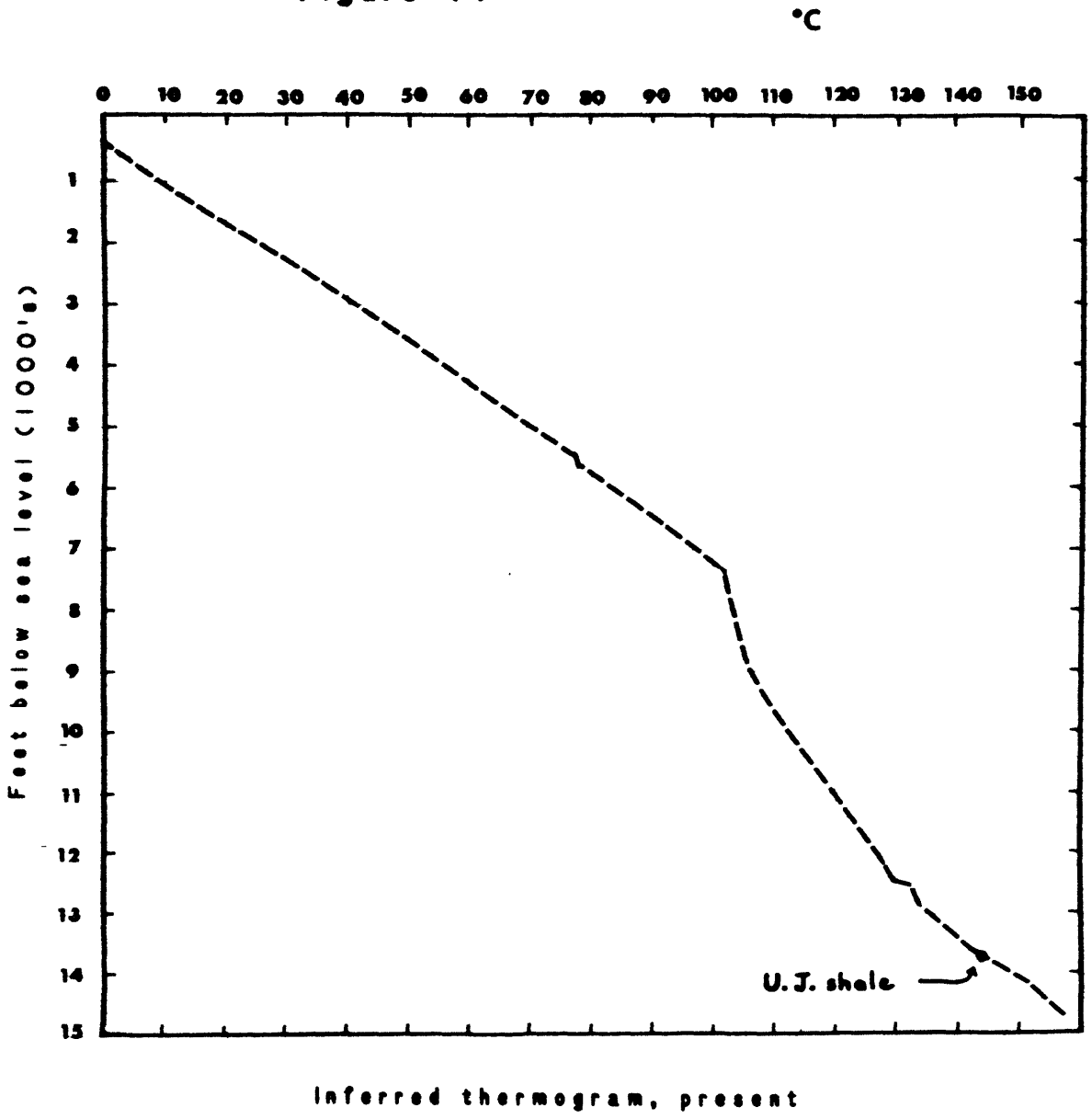
°C
0
10
20
30
40
50
60
70
80
90
100
110
120
130
140
150
1
2
3
4
5
6
7
8
9
10
11
12
13
14
15
Feet below sea level (1000's)
U.J. shale
Inferred thermogram, present

FIGURE II 3.

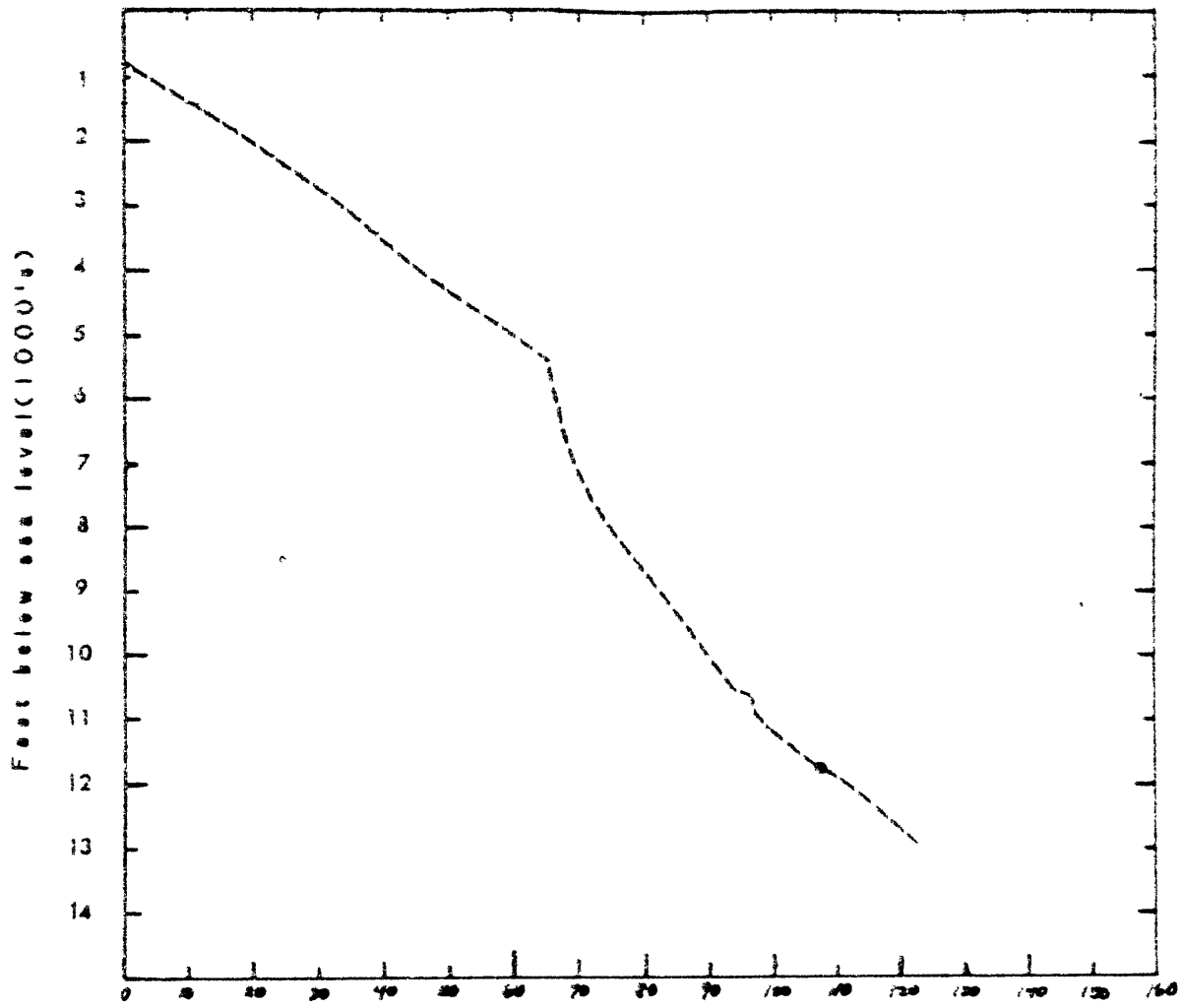

Palaeothermogram: 15 MYBP

FIGURE 11 C.

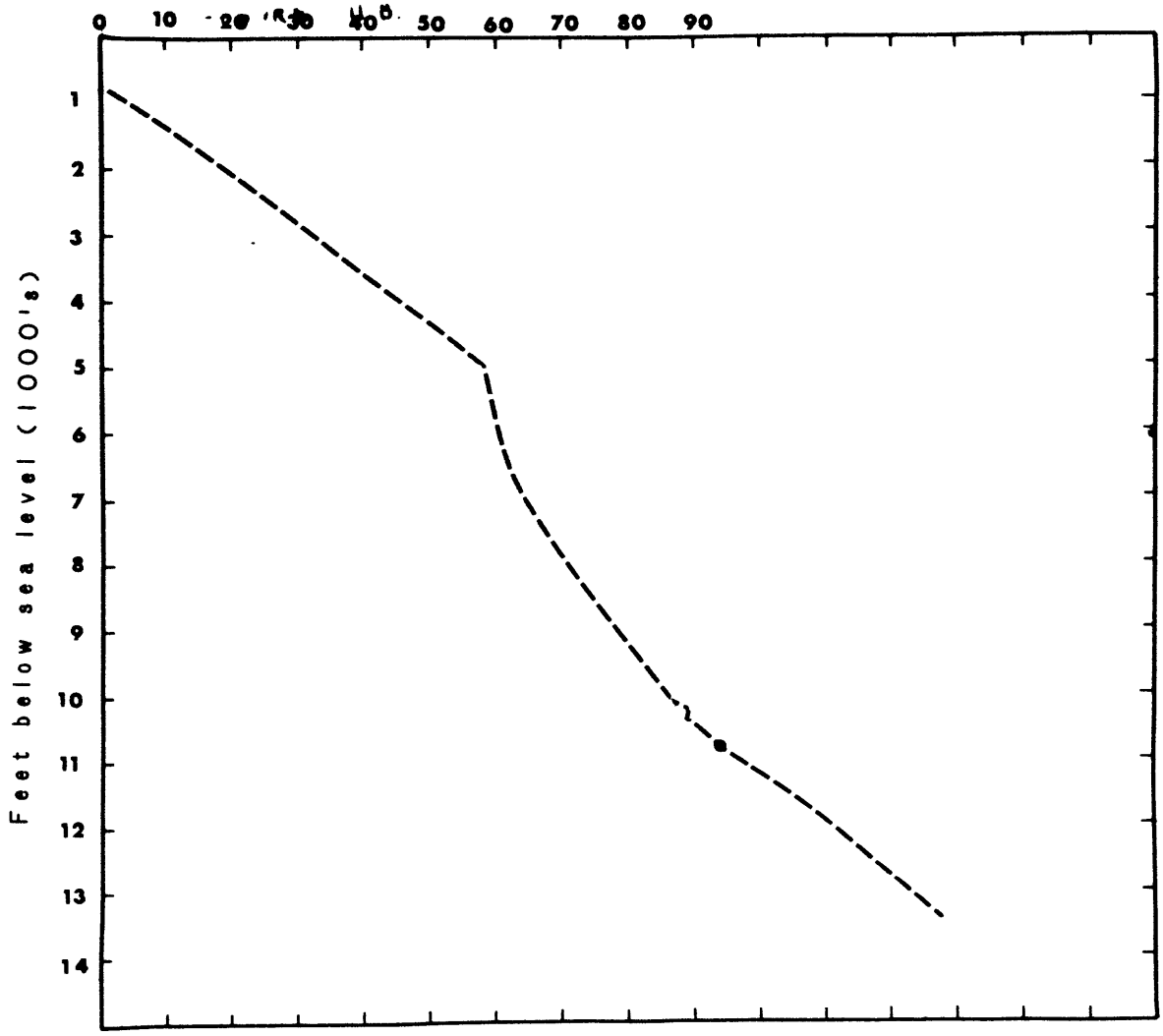

Paleothermogram: 21 MYBP

FIGURE II D

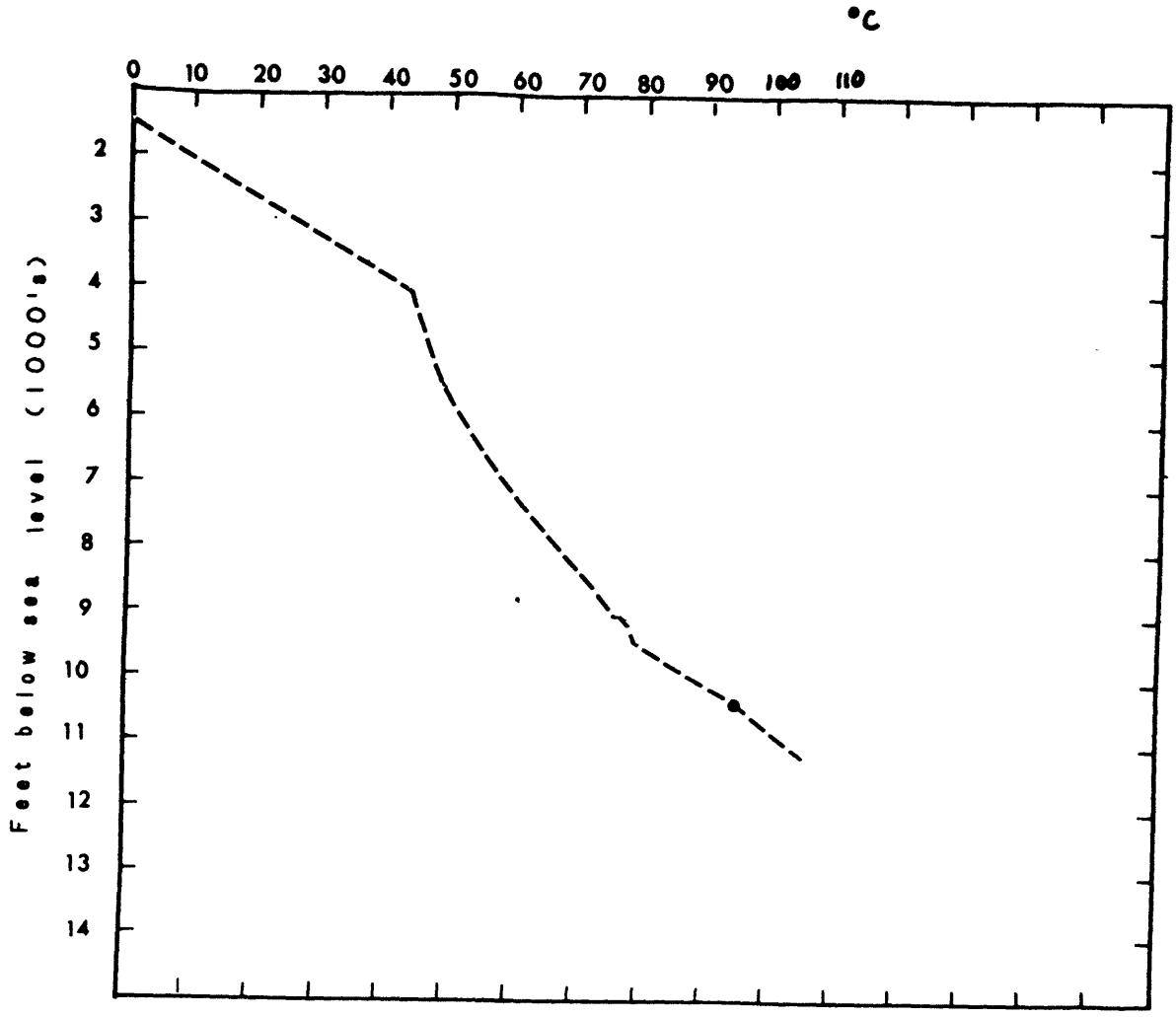

Paleothermogram: 36 MYBP

FIGURE II E.

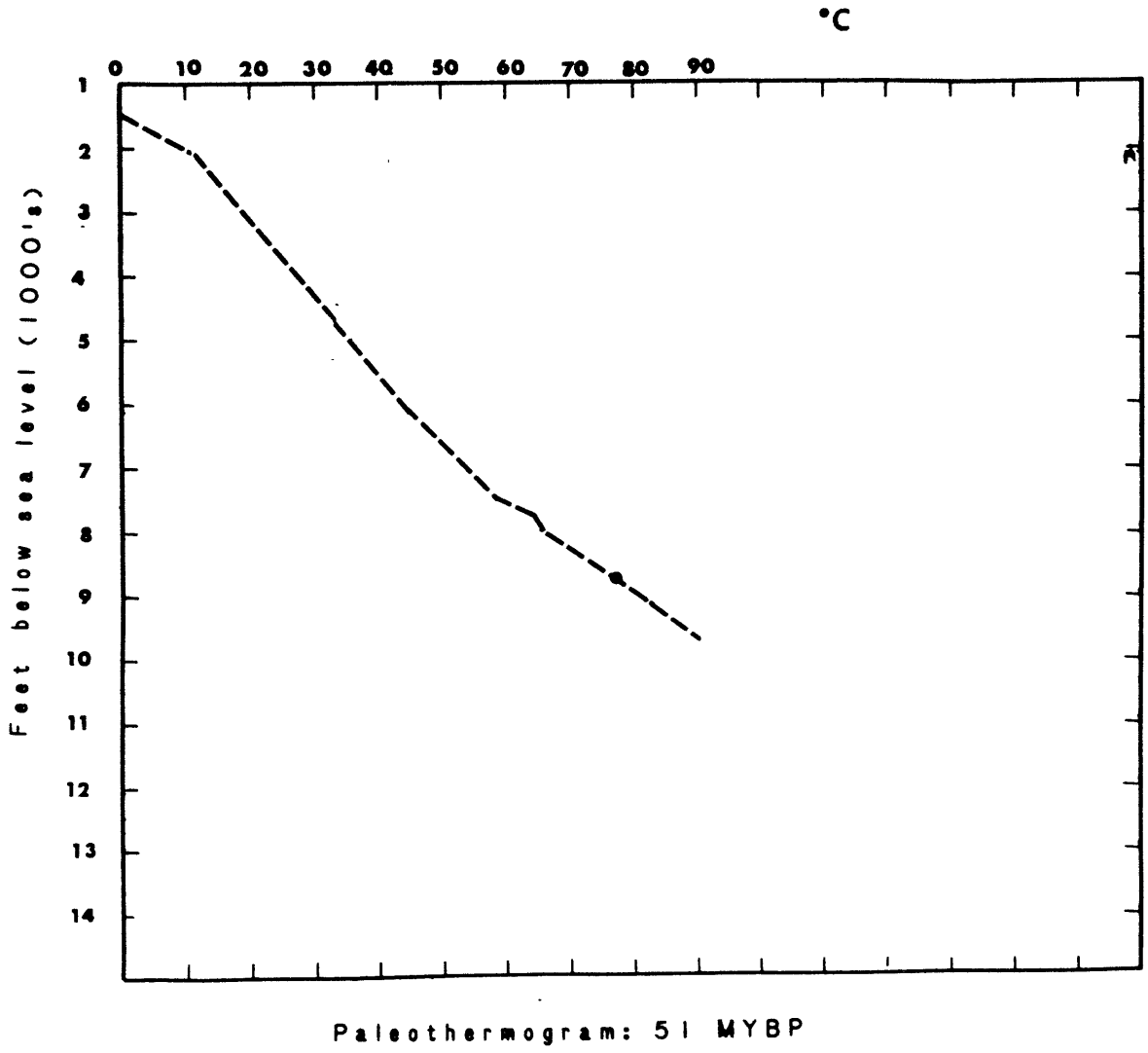

Paleothermogram: 51 MYBP

FIGURE II F

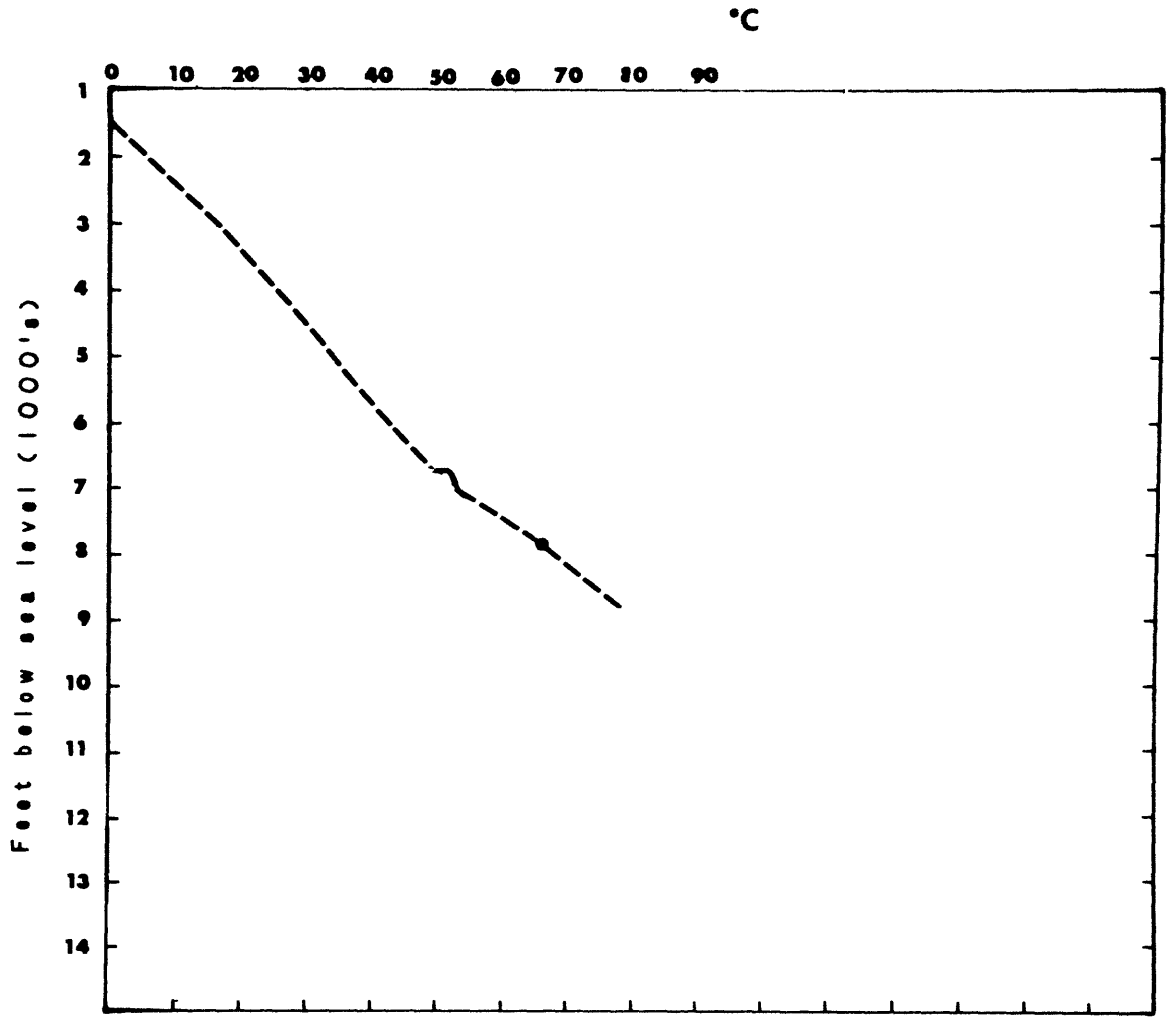

Paleothermogram: 56 MYBP

FIGURE 11 G

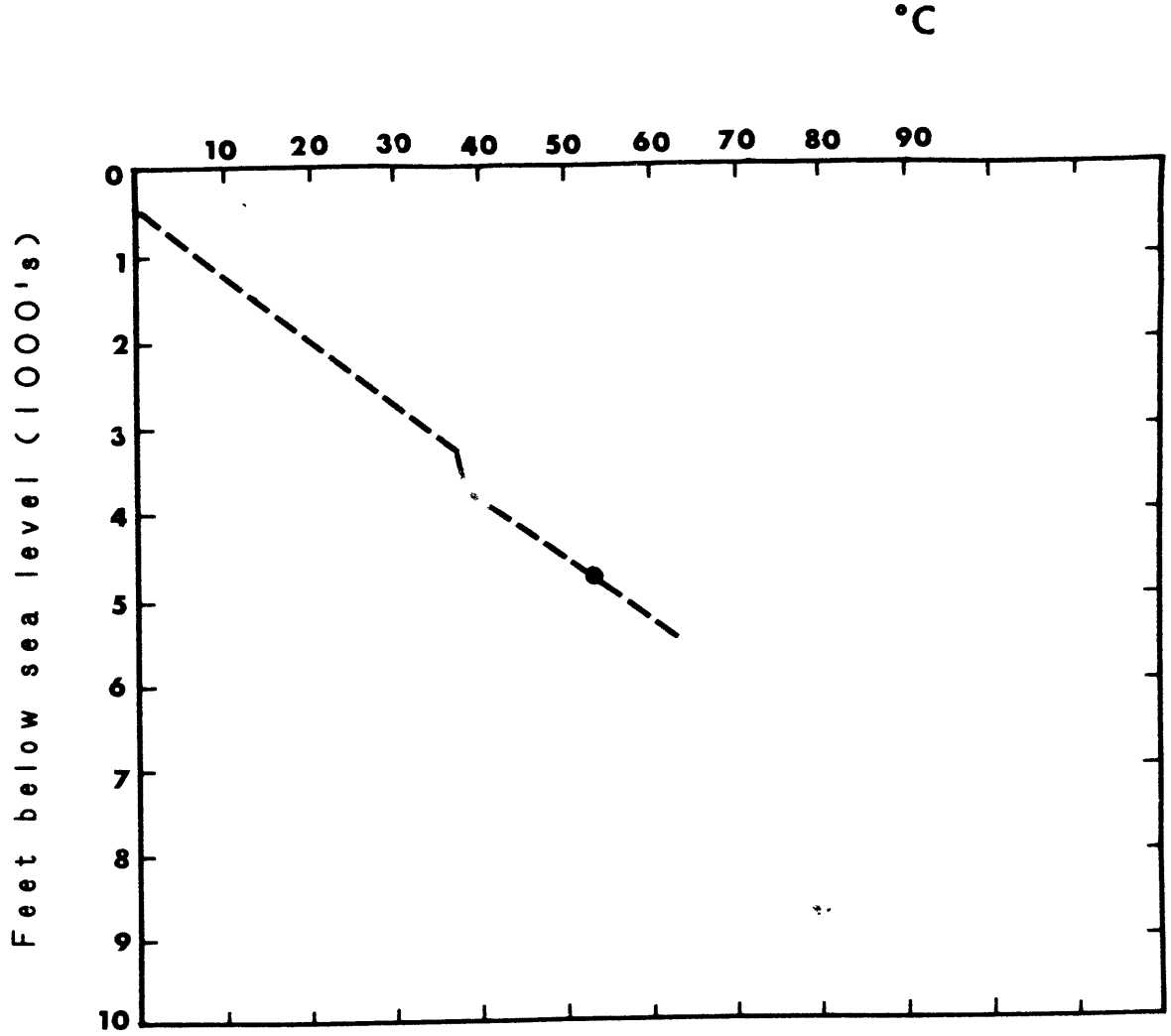

Paleothermogram: 75 MYBP

Figure 12.

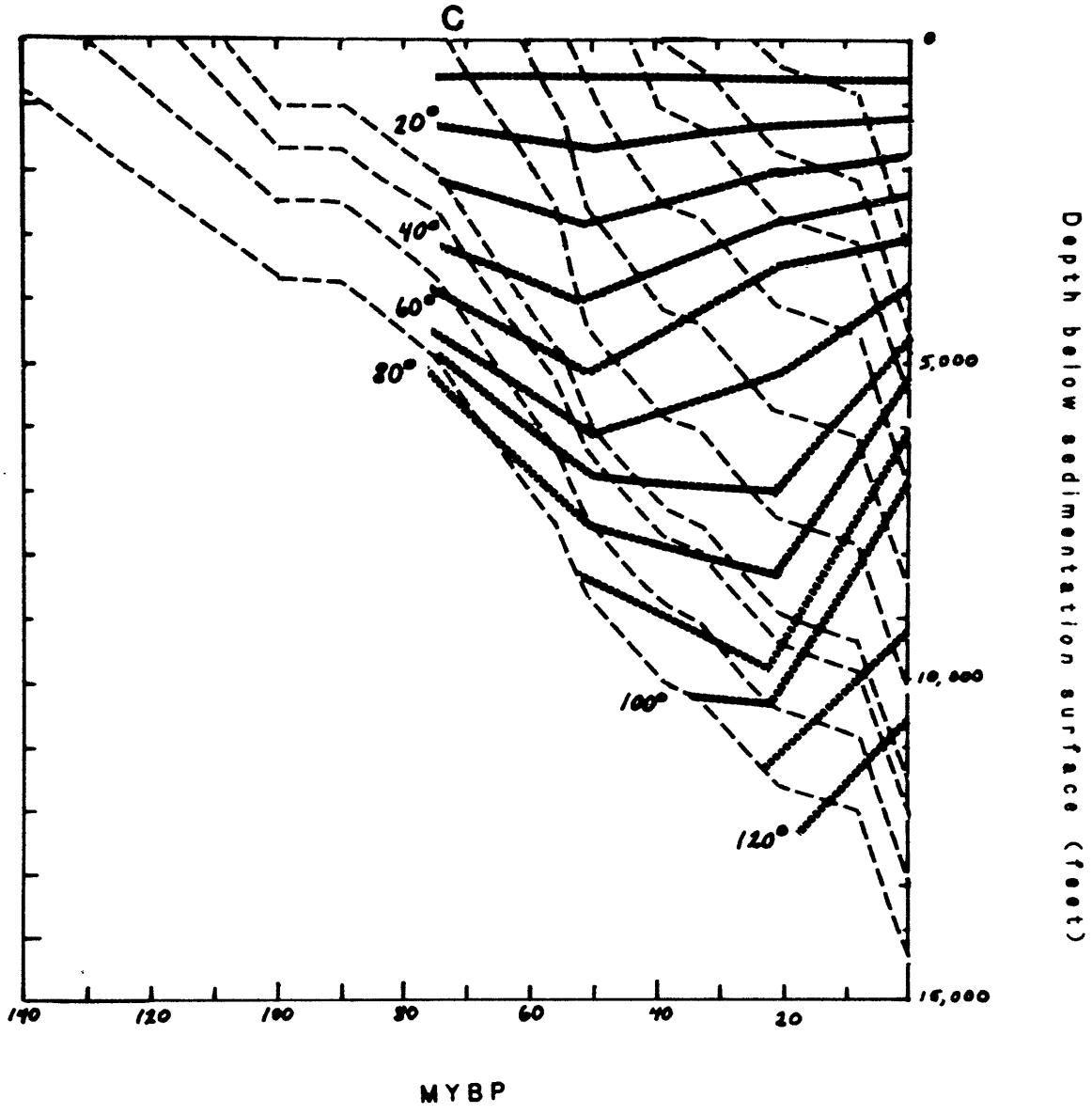
C
20°
40°
60°
80°
100°
120°
5,000
10,000
15,000
140
120
100
80
60
40
20
MYBP
Depth below sedimentation surface (feet)

Figure 13.

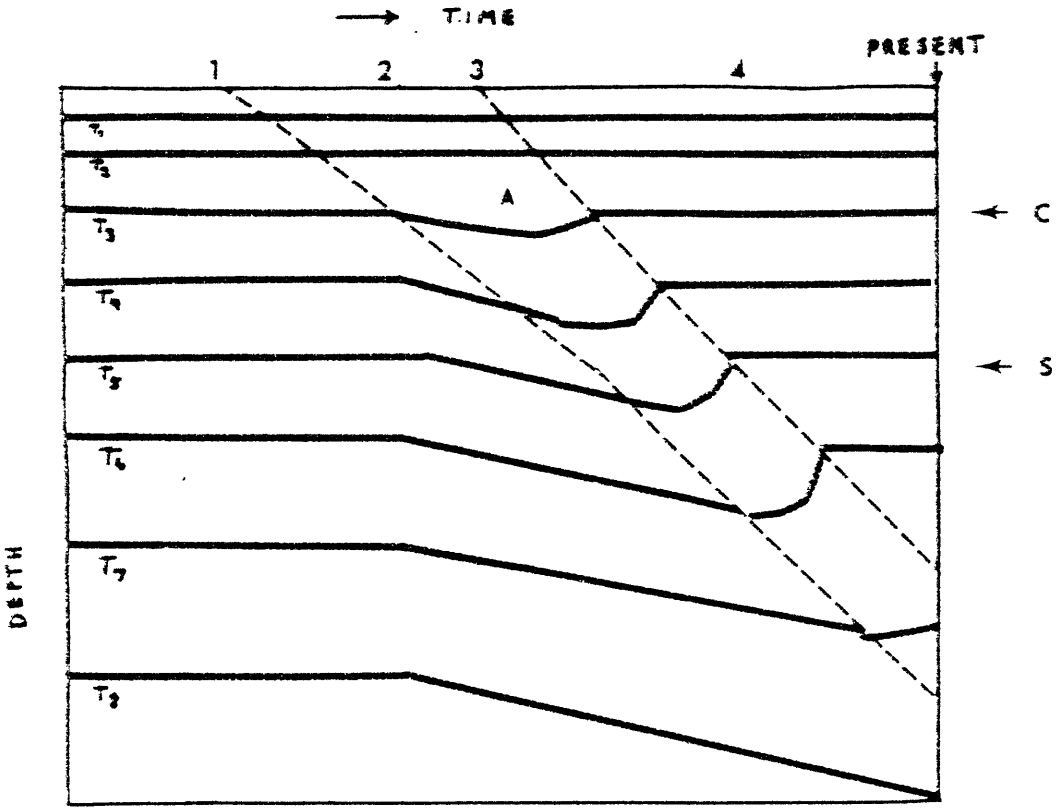

Subsidence and isotherm history (schematic) for a sedimentation sequence which includes a high (solid) conductivity layer, A, deposited between times "1" and "3". At time "2", base of A is at level C and begins to affect "normal" isotherms.

At time 4, all of the layer A is sealed and undergoes no further compaction. Its effect on the basin's thermal resistance is henceforth constant.

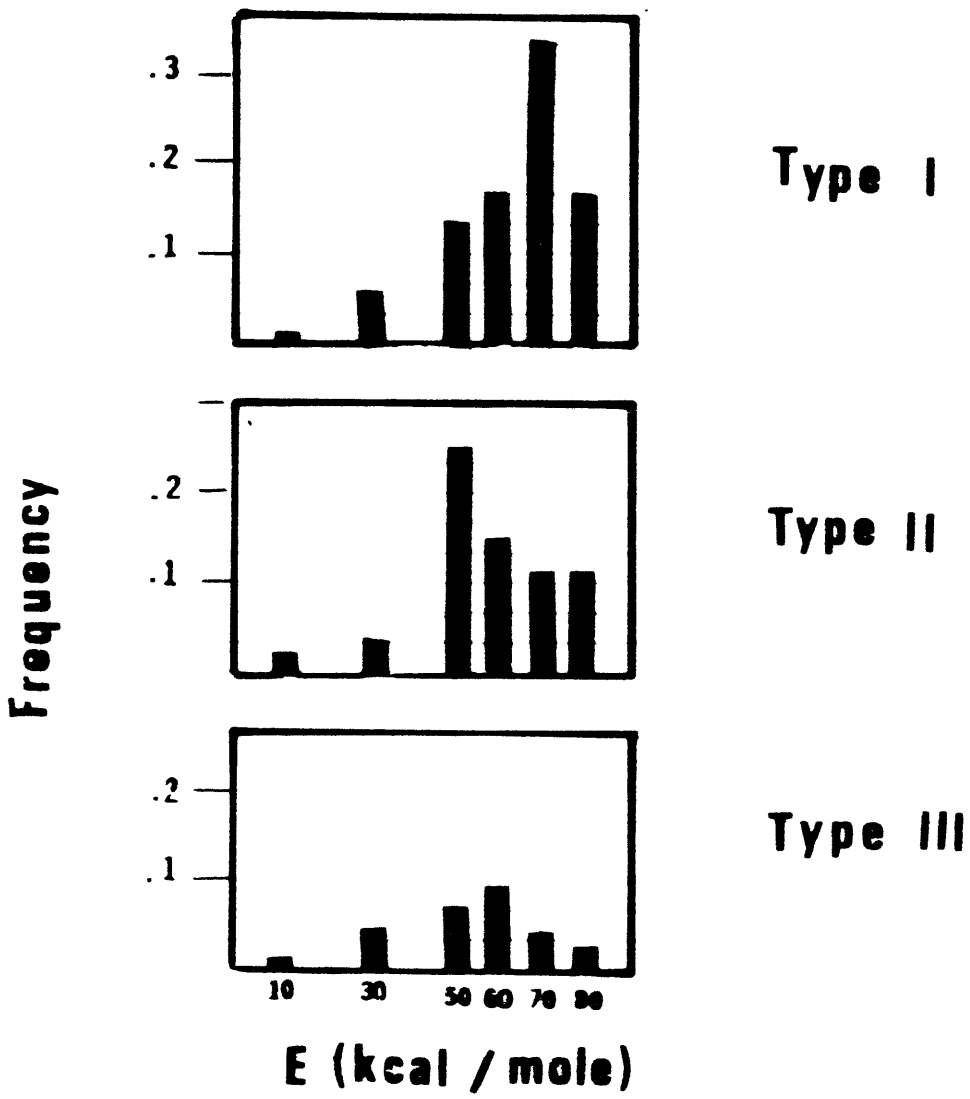

Figure 14.

After Tissot and Welte (1978)

Figure 15.

Thermal history of Upper Jurassic Organic shale

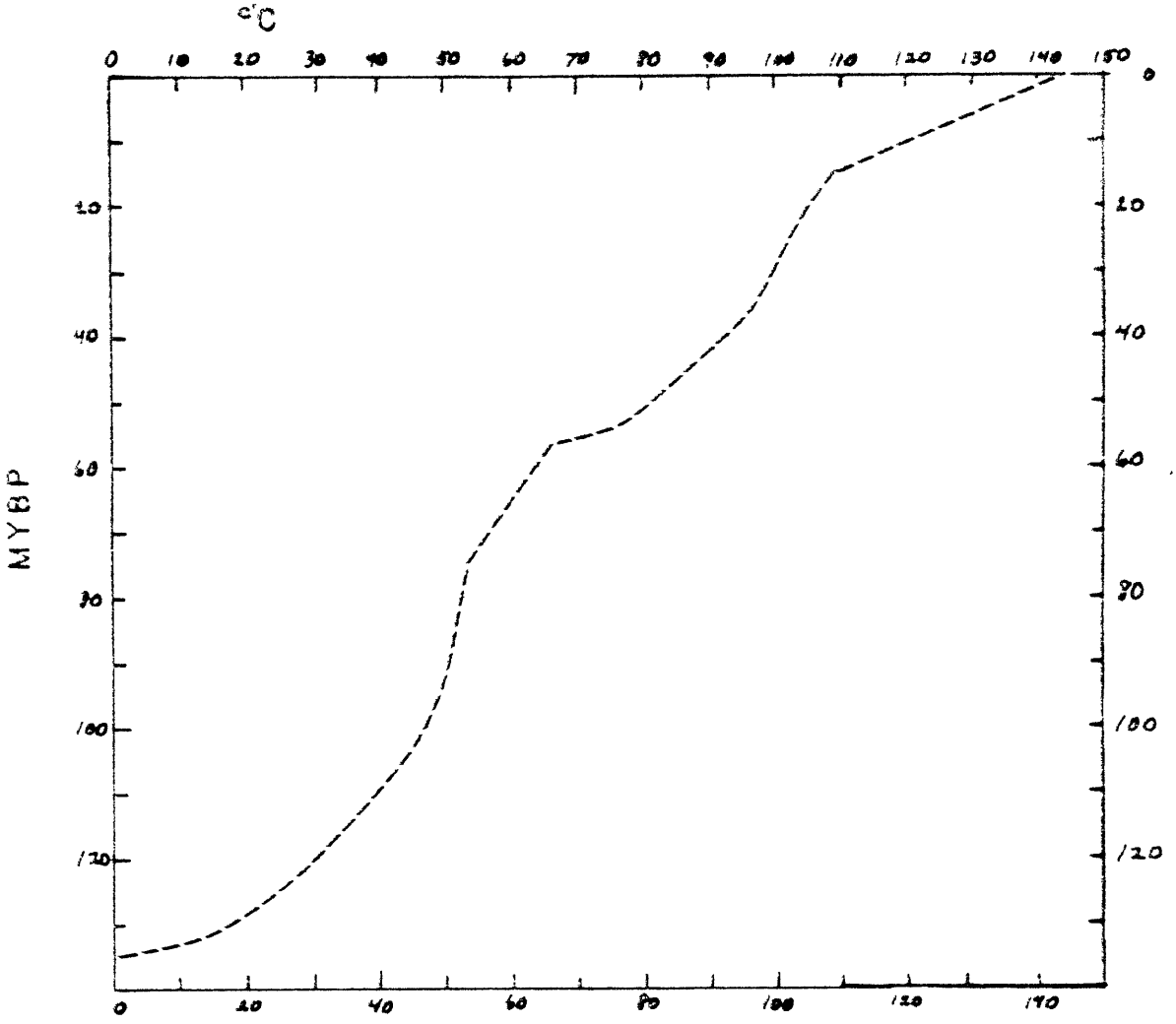

FIGURE 16.

TF / LOM